Atmos. Chem. Phys. Discuss., 12, 29967–30019, 2012
www.atmos-chem-phys-discuss.net/12/29967/2012/
doi:10.5194/acpd-12-29967-2012

Atmospheric Chemistry and Physics Discussions

Arctic aerosol life cycle: linking aerosol size distributions observed between 2000 and 2010 with air mass transport and precipitation at Zeppelin station, Ny-Ålesund, Svalbard

P. Tunved, J. Ström, and R. Krejci

Department of Applied Environmental Science (ITM), Stockholm University, 11418, Stockholm, Sweden

Received: 21 September 2012 – Accepted: 9 November 2012 – Published: 21 November 2012

Correspondence to: P. Tunved (peter.tunved@itm.su.se)

Published by Copernicus Publications on behalf of the European Geosciences Union.

Abstract

In this study we present a qualitative and quantitative assessment of more the 10 yr of aerosol number size distribution data observed in the Arctic environment (Mt Zeppelin (78°56′ N, 11°53′ E, 474 m a.s.l.), Ny Ålesund, Svalbard). We provide statistics on both seasonal and diurnal characteristics of the aerosol observations and conclude that the Arctic aerosol number size distribution and auxiliary parameters such as integral mass and surface have a very pronounced seasonal variation. This seasonal variation seems to be controlled by both dominating source as well as meteorological conditions in general. In principle, three distinctly different periods can be identified during the Arctic year: the haze period characterized by a dominating accumulation mode aerosol (March–May) followed by the sunlit summer period with low abundance of accumulation mode particles but high concentration of small particles which likely are recently and locally formed (June–August). The rest of the year is characterized by comparably low concentration of accumulation mode particles and negligible abundance of ultra fine particles (September–February). Minimum aerosol mass and number concentration is usually observed during September/October. We further show that the transition between the different regimes is fast, suggesting rapid change in conditions defining their appearance. A source climatology based on trajectory analysis is provided and it is shown that there is a strong seasonality of dominating source areas, with dominance of Eurasia during the autumn-winter period and dominance of North Atlantic air during the summer months. We also show that new particle formation events seem to be a rather common phenomenon during the Arctic summer, and this is the result of both photochemical production of nucleating/condensing species and low condensation sink. It is also suggested that wet removal play a key role in defining the Arctic aerosol year, and plays a crucial role for removal of accumulation mode size particles as well as it may play a pivotal role for facilitating the conditions favoring new particle formation events. In summary the aerosol Arctic year seems to be at least qualitatively predictable based

ACPD

12, 29967–30019, 2012

on knowledge of seasonality of transport paths and associated source areas, meteorological conditions and removal processes.

1 Introduction

The Arctic environment is well known to be particularly sensitive to perturbations of the radiative budget. During the last century the temperature increase in the Arctic has been observed to be two times larger than global average (IPCC, 2007). The reason for this "Arctic amplification" is not fully understood, but it likely relates to the complex feedbacks as well as the environmental conditions that are characteristic of the Arctic environment. The increased warming results in, e.g. earlier onset of sea ice melt and ice loss in general, which through positive feedback further impacts the radiative balance via reduced surface albedo (Hudson, 2011; Robock, 1983). Future changes in the Arctic are projected to progress rapidly: several studies have suggested that the Arctic Ocean may be seasonally ice free in next 30–40 yr (Serreze et al., 2007; Wang and Overland, 2009). This will have a larger impact also on atmospheric aerosol sources and sinks as well as on cloud properties and cloud distribution in the region.

Aerosols are key constituents of the atmosphere and they belong to a group of trace constituents called Short Lived Pollutants (SLP's). Aerosol particles are believed to perturb the radiative balance of the Arctic environment in numerous ways. During the last three decades, the Arctic environment has experienced a warming of $1.48 \pm 0.28\,^{\circ}\mathrm{C}$. Of this warming, $1.09 \pm 0.81\,^{\circ}\mathrm{C}$ have been attributed to changes in aerosol forcing (Shindell and Faluvegi, 2009). The climate influence of aerosol particles is on one hand a result of their ability to both directly scatter and absorb incoming shortwave solar radiation (Charlson et al., 1992). The former is assumed to result in a net cooling of the lower atmosphere and surface, while the latter may cause warming of the atmosphere and subsequently also the surface due to increased down-welling of long wave radiation. However, recent studies suggest that this may induce dynamic feedbacks that still lead to a net cooling of the surface due to weakening of lateral temperature gradients (Sand

ACPD
12, 29967–30019, 2012

et al., 2012). The ratio between scattering and absorbing chemical species, as well as particle size, and their abundance will determine the magnitude of the combined effect. Furthermore, aerosols do also constitute the seeds upon which cloud droplets form. Changes in the aerosol chemistry and abundance will indirectly affect the cloud microphysical properties (Twomey, 1977) and lifetime (Albrecht, 1989). The net effect of altered aerosol-cloud interactions over the Arctic remains uncertain, and will naturally vary with season and location (Lubin and Vogelmann, 2010; Hu et al., 2005). Arctic is a complex environment where, opposed to large parts of the world, the typical cloud properties together with bright ice- and snow-covered surface cause clouds to actually warm the surface by more efficiently trapping and re-emitting a portion of the outgoing long-wave radiation in the Arctic (Shupe and Intrieri, 2004; Garrett et al., 2002). This is in particular true during the dark winter period of the year. High sun and dark surfaces will favor shortwave forcing, whereas bright surfaces and low sun or darkness will favor the long wave radiation forcing.

Furthermore, absorbing species, such as soot, may boost surface heating and ice melting by decreasing the surface albedo when deposited on snow and ice (Rosen et al., 1981; Clarke and Noone, 1985; Hansen and Nazarenko, 2004) (Flanner et al., 2007). As indicated above, aerosols may substantially impact the radiative budget of the Arctic. Understanding the spatial and temporal variability of microphysical properties of the Arctic aerosol may provide one of the fundamental tools to determine the magnitude as well as direction of future climate change in the Arctic region.

The Arctic aerosol has been shown to be highly variable over the year. A prime example is the Arctic spring period when elevated concentration of aerosols and trace gases largely define the matrix of atmospheric trace constituents. This annually reoccurring phenomenon is called Arctic haze and was first observed in the 50's during routine flights over the Arctic (Mitchell, 1956). With its comparably high concentration of larger sized particles and mass, the Arctic haze period is in sharp contrast to the otherwise clean Arctic air (Shaw, 1995). The elevated particle and gas concentrations originates from lower latitudes, that as a result of strong inversions, hindered vertical

ACPD
12, 29967–30019, 2012

mixing, lack of formation of cloud systems together with atmospheric blocking phenomena are allowed to be transported into the Arctic region (Iversen and Joranger, 1985; Shaw, 1981). The haze particles mainly consist of sulfates and different organics constituents, with some additions of ammonia as well as soot and other trace elements, reflecting their anthropogenic origin (Quinn et al., 2007; Heintzenberg et al., 1981). Elevated concentrations of above mentioned species are often associated with increased concentrations of sulfur dioxide, nitric acid or PANs (Jaeschke et al., 1997; Jaeschke et al., 1999).

It is still debated how different natural and anthropogenic source regions contribute to the Arctic aerosol, Several studies on the topic have been performed utilizing transport climatologies and various statistical methods. One of the more recent studies is the works performed by (Hirdman et al., 2010) where the importance of source regions in characterizing some key SLP's at three Arctic sites (Barrow, Zeppelin and Alert) was investigated. The dominating sources of sulfate aerosols and equivalent black carbon in the Arctic during winter were argued to be northern parts of Eurasia, while summer time suggests important contributions from sources in Siberia and North America. Importance of biomass burning in Russia, Siberia and Kazakhstan as an important contribution to high springtime aerosol loadings in the Arctic has previously been demonstrated (Warneke et al., 2009). Eastern European agricultural fires were responsible also for,so far, record high air pollution levels in European Arctic observed in spring 2006 (Stohl et al., 2007). No direct evidence of important source contributions of black carbon from Asia or southern parts of North America could be found, although these areas could possibly, at least occasionally contribute with sulfur to the Arctic. Other studies of long term transport climatology include the works of (Brock et al., 2011; Polissar et al., 1998, 2001; Stohl, 2006; Fisher et al., 2010).

In contrast to the Arctic Haze period, late spring and summer aerosol properties are very different. Change in general circulation, increased presence of low level clouds and thus more effective wet removal result in rather fast clean up after the haze period. Lower aerosol loading, increased photochemistry and biological activity results in a

ACPD
12, 29967–30019, 2012

peak in new particle formation during Arctic summer (Strom et al., 2009; Engvall et al., 2008b). Where and how the new particle formation predominantly occurs is still under debate. Observations show new particle formation taking place at both higher altitudes including free troposphere (Weber et al., 2003; Khosrawi et al., 2010; Hegg et al., 1995) as well as in boundary layer near surface (Strom et al., 2009). Occasionally, long-range transport pollution events occur also during summer (Iziomon et al., 2006; O'Neill et al., 2008). The Arctic winter is devoid of sunlight, and typically, concentrations and variability of aerosols are low.

In this study we provide a compilation of ten years of aerosol number size distribution observations and characterize these with respect to seasonal and diurnal variations and source regions influence. We investigate and discuss the role of different processes controlling the aerosol size distribution on longer and shorter temporal scales. By performing trajectory analysis and transport statistics, we provide an explanation to the variability of the aerosol number size distribution as observed at Mt Zeppelin in terms of atmospheric aerosol source, sink and transformation processes.

2 Methods

2.1 Aerosol observations at Mt Zeppelin

The aerosol number size distribution observations that are presented in this study were collected at the Zeppelin observatory located on the top of Mt Zeppelin, Svalbard (78°56′ N, 11°53′ E, 474 m a.s.l.), just outside the small community of Ny Ålesund. The station represents remote Arctic conditions, and offers a unique possibility to study the characteristic features of Arctic atmospheric trace constituents such as trace gases and aerosols.

The Zeppelin observatory is mostly unaffected by local sources and is considered to be within the boundary layer most of the time. On occasions when the top of the boundary layer is below the station altitude, however, measurements can be consid-

ACPD
12, 29967–30019, 2012

ered to be representative of the lowermost free troposphere. The local wind pattern is dominated by east-southeast katabatic flow from Kongsvegen glacier (Beine et al., 2001). Orographic effects from surrounding hills can deviate local winds.

The observatory is owned by the Norwegian Polar Research Institute (NP), and the Norwegian Institute for Air Research (NILU) is responsible for the scientific program coordination. The Department of Applied Environmental Science, Unit for Atmospheric Science (ITM), Stockholm University, plays a key role in monitoring of atmospheric aerosols and has performed observations of the high Arctic aerosol at Mt Zeppelin since year 2000. It is one of the longest observational series of aerosol number size distributions in polar environments. Alongside with observations of the aerosol number size distribution, ITM further monitors the aerosol light absorption using a custom built Particle Soot Absorption Photometer (PSAP) and aerosol scattering coefficient using an integrating nephelometer TSI 3563. Total particle number concentration larger than 3 and 10 nanometers is measured by TSI CPC model 3025 and TSI CPC model 3010, respectively. In this study however, we will focus only on the aerosol size distribution properties.

The aerosol number size distribution is observed using a closed loop Differential Mobility Particle Sizer (DMPS). During the period of operation, the system has undergone some changes with respect to inlet design and type of DMA used in the system. When the measurements started in beginning of 2000, the system consisted of a CPC 3760 together with a short Hauke type DMA (Jokinen and Makela, 1997; Knutson and Whitby, 1975). Initially, the observations covered the size distribution between 22 and 500 nm. In October 2000, the size range of the instrument setup was adjusted to observe the size distribution between 20 and 630 nm. This set-up was used until the end of 2002, when the system was modernized and the short Hauke type DMA was replaced by a medium size Hauke DMA. Both setups used the same TSI CPC 3760, and the size range observed remained the same. From 2005 the aerosol size distribution size range was further increased covering particle sizes between 10 and 790 nm. During end of 2005, the rain cover on the inlet was also replaced. The last change affecting

ACPD
12, 29967–30019, 2012

the data dates to the end of 2008 when the sampling tubing was changed leading to reduction of the diffusion losses in the sampling line. This in turn increased the detection efficiency of the smaller sized particles.

Although the aim is to keep the measurement continuous, some gaps in the data set will inevitable occur due to measurement failure and other unforeseen events. Based on daily averaged aerosol size distributions, present data set covers 84 % of time from year 2000 to 2010 (Fig. 1). During the period of measurements presented in this study there are no large gaps in the data apart from three longer periods of missing data (cf. Fig. 1; autumn-winter 2002, winter 2004 and winter 2008–2009).

2.1.1 Inter-annual variability of recorded data

In order to assure consistency of the used data-set we performed a comparison of annually averaged number and volume distributions. Figure 2 shows the 25–75th percentile range of the bulk of size distribution observations performed during the period 2000–2010 (red surface) with overlaid annual median size distributions. It is evident that the annual median distribution of years 2000 and 2002 significantly differ from the rest. This is due to the fact that a large part of both these years are missing. For year 2000 the observations did not start until end of March and large parts of the data for 2002 is missing due to the instrument temporary being out of commission. Otherwise, the annual average distributions seem centered around the median of the whole measurement series. Figure 3 shows corresponding aerosol volume size distribution with upper and lower quartiles range and annually average values. Apart from the obvious outliers corresponding to 2000 and 2002 previously described, there is a shift in the volume distribution towards larger sizes going from 2000–2010. Whether this is a result of changed instrument setup or actual change of the Arctic aerosol size distribution due to changes in transport pattern and sources and sinks is however uncertain, and it deserves a more thorough analysis in future, as it is not within the scope of current study.

ACPD
12, 29967–30019, 2012

2.2 Lognormal fitting procedure

The data was fitted with three lognormal modes for the daily averaged data. Fitting was performed for size distribution data between 20 and 630 nm in order to assure that the analysis was performed on a data set with identical size range for the studied period. The modes roughly correspond to size ranges of the nuclei, Aitken and accumulation mode particles. The fit of 3215 daily average aerosol size distributions was performed based on the algorithm fmincon.m, available in Matlab Optimization toolbox.

2.3 Trajectory calculations

Throughout the studied period, hourly 240 h back trajectories were calculated using the HYSPLIT4 model (Draxler and Hess, 1993). Between 2000 and 2006, the trajectory calculations are based on meteorological data from the FNL data set and from 2007 onwards they are based on GDAS (Global Data Assimilation System) data set (cf. http://ready.arl.noaa.gov/archives.php). The trajectories will be used to estimate spatial distributions of the potential source areas that define the aerosol properties at Zeppelin. The same trajectories will further be used to study the air mass history in terms of precipitation intensity which is supplied as optional hourly output along the calculated trajectories.

3 Results and discussion

The purpose of this study is to analyze long term observations of the Arctic aerosol number size distributions towards better understanding of what processes control Arctic aerosol properties.

First a survey of the general aerosol size distribution properties observed between years 2000–2010 is presented. The second part will describe both seasonality of the aerosol properties and diurnal variability. The third part focuses on a study of air mass transport patterns using trajectory analysis and description of seasonal variability. Fi-

ACPD
12, 29967–30019, 2012

nally, in the last part, role of precipitation in shaping the aerosol size distribution in the Arctic environment will be analyzed and discussed.

3.1 Average size distribution properties of the Arctic aerosol

The Arctic aerosol concentration is generally very low, typically a couple of hundred particles per cm^{-3} (Strom et al., 2003). Also, both integrated aerosol mass and surface concentrations are very low compared to observations performed in, e.g. the close-by boreal region of Scandinavia (Dal Maso et al., 2007). Figure 4, shows the median aerosol number, volume and surface size distribution for the studied period March 2000–December 2010. The average number size distribution (Fig. 4a) is typically bimodal with two modes in Aitken and accumulation mode size range. On average, the accumulation mode number concentration dominates the aerosol size distribution, and peaks around 150 nm.

The aerosol surface distribution (Fig. 4b) is defined by roughly a single mode with the maximum peak located around 220 nm. The average volume size distribution (Fig. 4c) peaks at around 300 nm. There is indication of a second mode in aerosol volume distribution, but its peak is located above the upper limit of the measurement range and extends towards size around 1 µm or above.

Daily average aerosol number size distribution data have been fitted into three log-normal modes (cf. Sect. 2.2). In the forthcoming, we will use the terms nuclei, Aitken and accumulation modes for mode 1–3, respectively, although the mode 1 modal diameter is slightly too large to be called a nucleation mode. Nevertheless, this mode represents aerosol population in smallest observed sizes, which potentially originate from new particle formation that occurred rather recently (an assumption based on the fact that lifetime of such small particles is short). The aerosol number size distribution fitted modal parameters are summarized in Table 1. During the ten years of measurements in this study, the smallest mode is typically centered around 25–40 nm and have a number concentration around 5–36 cm^{-3} as indicated by the 25–75th percentile range. This low value is indicative of only small abundance of nuclei mode particles on

ACPD
12, 29967–30019, 2012

average. The second mode is typically located between 55 and 110 nm, with a modal concentration of 24 cm^{-3} as median. The accumulation mode is the most dominating mode, with typical median concentration of 37 cm^{-3} and modal size between 130 and 190 nm. As can be seen from the mean values in Table 1, episodically high particle concentrations in the different modes do occur, causing a more than double mean values compared to the median. These events are likely caused by either new particle formation events during summer (indicated by the comparably high concentration of nuclei mode particles) or episodes of long range transport (in the case of high concentration of accumulation mode). The fact that the mean concentration of the nuclei mode is higher than the 75th percentile of the data suggests a small number of cases with comparably high nuclei mode number concentrations. This pattern can be linked to seasonal variability in aerosol size distribution, which will be discussed in following section.

3.2 Strong seasonal variation of the aerosol size distribution properties

Figure 5 shows seasonal variation of the monthly median and mean integral aerosol number concentration of submicron aerosol particles from 20 nm to 630 nm in diameter derived from number size distributions for period 2000–2010. Overall, the aerosol number density, typically in a range from 50 to 200 cm^{-3}, is comparable to aerosol concentrations in coastal Antarctica (Koponen et al., 2003) and substantially lower than typical background aerosol concentrations in remote regions at lower latitudes where aerosol number concentration is usually between 300–500 cm^{-3}. The annual trend in Fig. 5 indicates clear and repeating strong seasonality in aerosol umber concentration. Minimum values are observed during autumn and onset of winter (ca 50 cm^{-3}). Maximum concentrations are observed during the summer months, with a monthly mean of 250 cm^{-3} during July. Although the seasonal variation of the integral number concentration seems to be virtually uni-modal, there are significant differences in the shape of the size distribution over the seasons, which are highlighted in Figs. 6 and 7. Figure 6 represent a spectral plot of the whole 10 yr period averaged on daily basis. The high

ACPD
12, 29967–30019, 2012

concentrations during spring months March–April are almost exclusively governed by the accumulation mode number aerosol, while the high summer concentrations are related to elevated number in the Aitken and Nuclei mode size ranges. Thus, the aerosol size distribution during the haze period appears to be dynamically aged, and represent the terminal stage of the aerosol lifecycle (e.g. Tunved et al., 2004). The summer period aerosol size distribution is dominated by (most likely) freshly formed particles that have not yet undergone significant growth by condensation and coagulation and have not been affected by cloud processing and wet removal. From this perspective it is a strikingly sharp transition between spring and summer periods, which represent a regime-shift between polluted spring and the relatively cleaner summer. The spring time domination of accumulation mode particles is diminished in favor of smaller particles over the time period of a couple of days. This phenomenon has been studied in detail by (Engvall et al., 2008b) using six years of aerosol size distribution observations from Mt Zeppelin. It was shown that the sharp transition between these two extremes happens every year during the same period, within a couple of weeks, and cannot be explained by changes air mass transport and source regions influence alone. Instead, this transition is associated with increased photochemical activity due to increased solar radiation. In combination with reduced condensation sink due to accumulation mode aerosol concentrations decrease, suitable conditions for new particle formation occur during Arctic summertime. This is of course dependent on a nucleating gas and its precursors could be either locally emitted, e.g. DMS from the ocean (Sharma et al., 2012) or, perhaps less likely, transported into the Arctic during certain transport conditions. Single particle analysis (Behrenfeldt et al., 2008) further indicated that samples taken before the rapid transition mainly consisted of spherical "organic like" particles originating from Eurasia, while particles sampled after the transition were more complex in nature with a higher influence of natural sources reflecting shift in general circulation within Arctic during transition from spring to summer period. Thus, while the spring maximum (i.e. "the Haze period") is linked to certain meteorological transport condi-

ACPD
12, 29967–30019, 2012

tions, the high concentration of small particles during summer likely reflect local new particle formation within the Arctic domain.

Figure 7 further emphasizes the seasonal variability in terms of monthly average aerosol number size distributions for the studied time period: the Arctic Haze period is dominated by an almost monomodal accumulation mode aerosol, which shift into a nuclei-Aitken mode size range dominated aerosol during the summer months. After the sun goes below the horizon after the summer, the size distributions again display more aged aerosol characteristics: the abundance of small particles decrease and relative fraction of accumulation mode particles increase. This trend and decrease in total aerosol number density continues throughout September and October when annual minimum in total aerosol number concentration is observed. From November the concentration of the accumulation mode aerosol slowly rise towards next year maximum during the following spring haze period.

This figure is accompanied by Table 2, providing monthly descriptive statistics for fitted aerosol number distributions. We will not address this table in detail, but do instead provide it for completeness as a reference for, e.g. model initialization and evaluation as well as for comparison with previously derived statistics from the Arctic environment.

Finally, Fig. 8, provides the seasonal variation of the integral mass ($\mu g\,m^{-3}$) and surface ($cm^2\,m^{-3}$). The mass is calculated from the submicron aerosol number size distribution simply assuming a density of $\rho = 1\,g\,cm^{-3}$ for ease of scaling (n.b. that dry aerosol densities are likely to be closer to $2\,g\,cm^{-3}$). The winter months are, as previously mentioned, characterized by very low aerosol concentrations, with a dominance of accumulation mode sized particles. Minimum mass concentrations are observed during September, whereas lowest number concentration was found in October. Not surprisingly, the maximum mass concentration is largest during the Arctic Haze period. Although relatively high for Arctic conditions, the maximum mass (around $0.8\,\mu g\,m^{-3}$) is small compared to continental sites (cf. with, e.g. Van Dingenen et al., 2004). The annual variation of the integral surface concentration follows approximately the same

ACPD
12, 29967–30019, 2012

pattern as the integral mass, but it is associated with a less pronounced spring maximum.

In summary, the Arctic boundary layer aerosol seems to be predictable and repetitive with respect to the aerosol size distribution seasonality trends and properties. Typical phases of the observed aerosol number size distribution can be characterized by three significantly different states: (1) the summer period, with its dominance of smaller sized particles, (2) the dark winter period with comparably few particles and dominance by accumulation mode sized particles slowly increasing in number, and (3) the Arctic Haze period with highly elevated concentrations of accumulation mode aerosol and just a few nucleation and Aitken mode particles. The timing of the transition between different characteristic aerosol regimes is, based on this and previous studies (Engvall et al., 2008b), consistent and very well pronounced.

3.3 New particle formation in the Arctic: diurnal characteristics of the Arctic aerosol number size distribution

So far, we have focused on the seasonal properties and variation of the aerosol number size distribution. While the annual variability most likely reflect the large scale features of Arctic meteorology and transport conditions, diurnal variability will reflect process active on a much smaller temporal and spatial scale. One such phenomenon is new particle formation. New particle formation (Kulmala and Kerminen, 2008), is occasionally observed also in the Arctic environment. Figure 9 provides an example on how these events look when observed at the Zeppelin site. The new particle formation events observed at Mt Zeppelin exhibit several general features: (1) They occur during the sunlit period of the year (i.e. summer months May–August), (2) they are detected around midday and (3) the newly formed particles seem to grow relatively slowly compared to other observations of new particle formation outside the Arctic. Many times, however, new particles are observed to appear, but without traceable growth. In this study we will not provide a detailed inventory of the nucleation events in terms of classification,

ACPD
12, 29967–30019, 2012

growth rate and formation rate. Provision of similar analyses will be in future studies. Instead, we focus on more general diurnal trends of the Arctic number size distribution.

The dataset including data from 2000–2010 was split into 12 monthly subsets and these monthly subsets were further sorted according to time of day and then averaged. This gave a monthly average diurnal variation for the studied decade. Firstly, when investigating median integral number concentrations, there was no evident diurnal variability. From this we draw the conclusion that there is no typical systematic diurnal variation of neither of the studied size classes on a day-to-day basis. In order to highlight any diurnal variability that may be hidden in the dataset, hourly 5th and 95th percentile ranges were calculated. This will reveal the more extreme cases in the dataset and how these extremes in turn will vary on shorter time scales. Figure 10 shows monthly median and 5–95 percentile rages of the sub 60 nm and super 60 nm integral particle population. The selected cutoff of 60 nm is based on the on average shape of the size distribution, consisting of a mode above 60 nm and mode below 60 nm, with a typical Hoppel minimum (Hoppel and Frick, 1990) in-between (cf. Fig. 4). Except for the period June–August, when both the sub-60 nm and the super-60 nm particle populations are of similar magnitude, median concentration of the sub 60 nm population is always lower than the integral of the larger size classes.

There is only little or no diurnal variation observed for the larger particles. This suggests that the super-60 nm accumulation mode aerosol particles number concentration is controlled by long range transport, and does not seem to be systematically affected by processes acting locally and on shorter time scales. The population of sub-60 nm particle concentration does seem to have a clear diurnal variability during Arctic summer, in particular June, July and August. The concentration of these particles increases around noon and start to decrease again during late afternoon. One plausible explanation for this would be vertical mixing with free tropospheric air reaching a maximum during midday resulting in elevated particle concentration. This, however, would only be true if two conditions are fulfilled: firstly, the vertical gradient of super-60 nm particles is small through whole tropospheric column since no diurnal variability is identified for

ACPD
12, 29967–30019, 2012

this size range. Secondly, particles are formed aloft. Concerning the first assumption, accumulation mode aerosol shows nearly homogeneous distribution through Arctic troposphere (Engvall et al., 2008a) including also not all, but some of the Arctic Haze occasions and plumes (Schmale et al., 2011). Regarding the location of particle formation, it is indicated by airborne measurements (Engvall et al., 2008a) that new particle formation in the free troposphere seem to be very rare in the Arctic. Instead, the shape of and continuity of the observed events (cf. Fig. 9) in many aspects resemble previously reported boundary layer nucleation events (Kulmala and Kerminen, 2008). The continuity (i.e. possibility to follow the evolution of the nuclei mode for several hours) further suggests that observed Arctic particle formation events are likely to take place simultaneously over large areas.

The data was further subdivided according to month, and average diurnal behavior of the full size distribution was calculated to reveal any systematic variation of the size distribution as whole over a 24 h cycle (Fig. 11). During January–February the average day is characterized by a persistent accumulation mode and there is no evidence of any diurnal variation of the aerosol number size distribution. Entering March, the lack of diurnal variability continues, but as this is one of the more prominent haze months, the number concentration of the accumulation mode is higher. All these months are as good as completely devoid of direct sunlight, although the sun rises towards the end of March. Entering April, the concentration of accumulation mode particles remain high an there seem to be an increased abundance of small (< 20 nm) particles having a maximum concentration around noon. In May this picture is even more pronounced, and there seem to be on average a formation of small particles around noon which seem to grow during the afternoon. In June, as previously described, the Haze disappears which means that the amount of accumulation mode particles is lower. During this month there is a persistent mode present in the Aitken size range and there is clear evidence of new particle formation starting to be visible around midday, followed by growth which is visible also during the following day. The sun is now high and the Arctic environment is characterized by constant daylight. This picture is preserved and

ACPD
12, 29967–30019, 2012

enhanced during the following months July–August, where the average data show typical signs of new particle formation and growth. Entering September, the sun sets and the signs of nucleation are diminished. This continues to be the case during the rest of the dark winter months, even though the amount of larger particles remains low.

We interpret this characteristic seasonal dependence as follows: During March–May, there is sunlight but also a large preexisting surface. The waters are mainly covered by ice. This means poor conditions for new particle formation as newly formed particles are scavenged quickly as are any potential nucleating gases (which in any cases likely are produced at a slow speed due to the lack of significant insolation). If the source of the precursor gases is the ocean itself, any emission of such is likely hindered by the ice cover. During June, conditions are quite different. More sunlight and less abundant preexisting accumulation mode particles means that the newly formed particles are able to grow into a large enough size that the particle lasts into the following day. On average any diurnal variation in Aitken mode particles is therefore masked. This is a feature shared by July and August months as well. These months are all characterized by high insolation, low aerosol surface (and mass) and a much higher fraction of open ocean. In September, as days become shorter and solar radiation decreases, the particle production ceases and period of dominating accumulation mode is reestablished. This again indicates the importance of photochemical production as the main driver for new particle formation in the Arctic environment.

The features associated with the diurnal characteristics of different size classes presented above support the idea that new particle formation in the Arctic boundary layer seems to be an important source of submicron particles during the polar summer. This corroborates earlier findings by, e.g. (Strom et al., 2003, 2009; Shaw, 1989). The qualitative and quantitative behavior of the temporal evolution of small particles show a behavior consistent with new particle formation events as observed at continental sites, and is further indicative of the important balance between generation of nucleating and condensing vapors on the one hand, and sink from making new particle material on the other hand (e.g Kulmala and Kerminen, 2008). This picture also holds for the general

ACPD
12, 29967–30019, 2012

features of nucleation events observed in the Arctic (i.e. detection of 10 nm particles around noon, which by assuming a growth rate of 2 nm per hour would have been formed some 5 h earlier), followed by growth that by its nature suggest condensational processes to be dominating (e.g. Dal Maso et al., 2005). Where exactly new particle formation takes place, what gaseous precursors are critical for aerosol nucleation and if these gaseous precursors dominantly are of natural or of anthropogenic origin remains to be addressed by future research.

3.4 Strong seasonal variation of source areas: monthly transport climatology for years 2000–2010

It has been shown earlier that the Arctic aerosol size distribution properties and diurnal behavior exhibit strong seasonal variability. To a certain degree we have already discussed the role of meteorological parameters such as intensity of sunlight, balance between generation and consumption of condensable gases, growth and potential sources. We have however not yet in detail discussed the role of the actual aerosol sources and source areas and their seasonal variation. Arctic air mass source climatologies focusing mainly on the Arctic Haze phenomenon are not something new, and detailed analysis regarding transport characteristics and source dependence may be found elsewhere (e.g. Hirdman et al., 2010; Polissar et al., 2001; Shaw, 1981). These and similar studies mainly address the source dependence of chemical composition and general meteorological characteristics. Here we will address source regions and transport patterns for air masses reaching Zeppelin station, by calculating relative horizontal source contribution based on trajectory calculations using the HYSPLIT model (c.f Sect. 2.3). We will investigate how the transport history is described in terms of source area and precipitation how the air mass history to a large degree defines the properties of the aerosol number size distribution.

Figure 12 shows the distribution of potential source areas experienced by a randomly selected trajectory during each month (frame 1–12) through the studied 10 yr period. Every map is generated by examining in what grids any single trajectory have resided

ACPD
12, 29967–30019, 2012

prior arrival. This is performed for every hourly trajectory calculated 2000–2010. Only the horizontal transport is considered, and we do not discriminate whether or not the trajectory is more or less close to the ground. After adding the number of hits in each grid, the matrix was divided by the total number of trajectories investigated for the month at hand. This results in a likelihood frequency that transport takes place from or over each one of the grids. The grid system itself is made up by 30 × 30 (3° Latitude and 12° Longitude) polar grids distributed around the receptor (Zeppelin). It is well known fact that the accuracy of the trajectories deteriorate rapidly with increasing transport distance (Engstrom and Magnusson, 2009). For this application, i.e. when using a very large number of trajectories, we do however believe that sufficient amount of information is retained by the individual trajectories to support the statistical analysis presented also when long transport time/distance is considered.

Starting with the Arctic Haze period, there seems to be a strong probability of transport of air over the Arctic ocean, and a majority of trajectories are arriving within an approximately 120° sector extending to Alaska in easterly direction and Northern Siberia in the westerly directions (cf. frame 3–5 for March, April and May data). Transport from continental sources seems to be dominated by transport from Siberia, Eurasia and to some degree the European subcontinent. Only minor parts of the 240 h trajectories extend down to East Asia and Central Asia. There is further a minimum influence of air mass transport over the Atlantic Ocean. Entering June, this pattern starts to break up. The dominating transport sector defining the haze period is weakened and a much larger portion of air is funneled over the Northern Atlantic Ocean.

During the following months July–August this pattern gets even more pronounced, suggesting that the source areas experienced during the summer period is substantially different from those experienced during the haze. Frames 6–8 in Fig. 12 suggest that a majority of air mass transport goes along two separate branches: one south-west of Greenland and one branch arriving from the north-west, north of Greenland. During September the transport patterns shift once more, and under the period October–

ACPD
12, 29967–30019, 2012

December is consistent transport through the Arctic from Eastern Siberia–Alaska. January and February is strong shift westwards in source regions.

Thus, in simple terms it seems so that transport in terms of geographical origin is defined mainly by two different patterns: Atlantic air arriving from the south west during the summer months and air mass transport over the Arctic ocean from Siberia, Eurasia and partly Asia during the rest of the year. In terms of the summer period compared to the rest of the year, the transition between aerosol properties seem somewhat straightforward as the air mass transport patterns are significantly different between these two periods. We note that although the transport patterns are similar for October and March, their respective aerosol characteristics are very different. These results should be compared to, e.g. the findings by (Hirdman et al., 2010) where the importance of source regions in characterizing some key SLP's at three Arctic sites (Barrow, Zeppelin and Alert) was investigated. The dominating sources of sulfate aerosols and equivalent black carbon in the Arctic during winter were argued to be northern parts of Eurasia, while summer time suggests important contributions from sources in Siberia and North America. Importance of biomass burning in Russia, Siberia and Kazakhstan as an important contribution to high springtime aerosol loadings in the Arctic has previously been shown by (Warneke et al., 2009).

In order to better understand how transport over different source regions may affect the aerosol properties in the Arctic, we also calculated maps showing the aerosol mass concentration observed on average after the air has crossed a certain grid. The aerosol number size distribution data was divided into hourly averages. For every average, the integral aerosol mass was calculated. For every one of these averaged observed mass concentrations, hourly backward trajectories were calculated.

These calculations are performed on monthly basis for the whole period 2000–2010. In simple terms, the mass concentration observed at Zeppelin during every hour is assigned to the grids crossed by the corresponding air mass trajectory. Performing this analysis for every trajectory and normalizing the result by the number of times a trajectory actually have crossed any particular grid square provides a measure on how

ACPD
12, 29967–30019, 2012

much mass on average is observed at the receptor (Zeppelin) after the trajectory has crossed any of the respective grids. The resulting plot is displayed in Fig. 13. The figure shows the mass concentration in $\mu g\,m^{-3}$ of integrated aerosol mass (20–630 nm) on average observed when a trajectory has crossed a particular grid.

Transport from Central Europe and Russia (including Siberia) and northern parts of Asia provide the conditions for observation of relatively high mass concentration in at the receptor Mt Zeppelin for all months. While this is true, it also becomes clear the mass concentration assigned to these source regions do vary substantially comparing the different months. For example, transport over Eastern Siberia during March results in observed concentrations of about 0.4–0.5 $\mu g\,m^{-3}$ while during September, the same area results on observed concentrations in the range of 0.1 $\mu g\,m^{-3}$. If we assume that the chosen approach at least to some degree represent the strength of the source areas, these results indicate that either the source strength changes substantial over the year or that the sinks during transport is significantly different comparing the different months.

The submicron aerosol mass is almost exclusively governed by accumulation mode particles (Fig. 4). As described in (Sect. 1) meteorological characteristics do play an important role in defining the seasonality of the Arctic aerosol. Furthermore, the most important sink for accumulation mode particles is wet removal (Buatmenard and Duce, 1986; Textor et al., 2006).

Thus, average amount of precipitation experienced per month during the studied period was calculated. This was done by integrating precipitation intensity calculated by the HYSPLIT4 model along the trajectories and averaging the result per month for the studied period. The result is presented in Fig. 14 as monthly median amount of accumulated precipitation during last 10 days (240 h). There is a strong annual variation in accumulated precipitation. Maximum values are estimated for the summer (7–8 mm_{tot} during July–September) months, and this amount gradually decrease during autumn, winter and spring to reach a minimum value during the haze period March–May (2–3 mm_{tot} during March–May). The fact that the minimum agrees well with maximum in

ACPD
12, 29967–30019, 2012

aerosol mass concentration do suggest that precipitation does play a key role for abundance and annual variability of the observed Arctic aerosol properties. In the following section we will therefore adopt a statistical approach to investigate how precipitation and wet removal could contribute in shaping the Arctic aerosol size distribution properties.

3.5 Precipitation: both sink and source of Arctic aerosols?

In order to resolve the potential importance of wet removal for shaping the Arctic aerosol, hourly values of precipitation intensity were extracted along each single trajectory and integrated during the full duration of transport for every trajectory. Integral precipitation during transport was compared to the observed mass concentration at the Zeppelin station. Subsequently, the integral precipitation was grouped according to amount of accumulated precipitation over the range of precipitation values using an increment of 0.5 mm per step. The corresponding mass was simultaneously calculated for every bin as 25th, 50th and 75th percentiles. The result is shown in Fig. 15.

It is seen that the mass versus precipitation follows an exponential function, with an initially rapid decrease in mass, followed by a decreased apparent removal rate when the accumulated precipitation is large and mass is small. At zero mm of accumulated precipitation, the typical mass concentration observed at zeppelin station is around $0.45\,\mu g\,m^{-1}$ (covering a typical range of 0.18–0.62 as indicated by the 25th–75th percentile range). The mass concentration drops comparably fast up to about 10 mm of integral precipitation. When accumulated precipitation during the transport is larger than 10 mm decrease in aerosol mass with precipitation is less obvious until there is no apparent change of aerosol mass with increasing precipitation.

In order to better resolve how precipitation influences the Arctic aerosol, a separate study was also performed to resolve how the wet removal affects the whole size distribution range and not only mass. Thus, in same manner as for the mass, each hourly observed size distribution was associated with precipitation history during transport.

ACPD
12, 29967–30019, 2012

The result was binned according to incremental accumulated precipitation (0.5 mm) during transport. The result is shown in Fig. 16.

First of all, there is initially a rapid decrease of larger sized particles. Assuming in-cloud scavenging to be the most important mechanism of removal, precipitation will remove the larger particles first and the removal will affect smaller and smaller particles as soon as the larger ones have been removed. This is, at least conceptually, sound considering the mechanisms and process active in activation scavenging (Guibert et al., 2003; Snider et al., 2003). The best CCN's will be consumed first, and as the number and size of the accumulation mode decrease, smaller and smaller sizes become activated since there is less competition for the available super-saturation. Considering several consecutive precipitation events, the cloud droplets will be bigger and bigger for every cloud cycle if we assume same dynamic forcing during the formation of the cloud (i.e. updraft, temperature, pressure and constant liquid water content (LWC)), and less particle number and mass will be removed per mm of rain as the size distribution is shifted towards smaller and fewer available CCN's. This mechanism is in qualitative agreement with the result presented in Figs. 15 and 16 (assuming that coalescence processes are the dominating mechanism of rain formation).

Secondly, after about 15–20 mm of total accumulated precipitation an apparent increase of nuclei and Aitken mode particles seem to take place. This could either be a result of different meteorological conditions and transport conditions during occasions of high precipitation resulting in contributions from different source areas and/or different source strength (e.g. increase in wind speed may result in larger emissions of both DMS and sea salt particles). That is, a mixture of conditions that result in the observed pattern. Another potential explanation is that the wet removal result in reduced mass and aerosol surface (i.e. reduced condensation sink) leading to higher concentration of gaseous precursors suitable for nucleation and new particle formation. This fits snugly with the previous discussion in Sect. 3.3 indicating a strong inverse relation between pre-existing amount of aerosol surface and new particle formation. If the latter is true, the apparent increase of smaller sized particles would be present only during the sunlit

ACPD
12, 29967–30019, 2012

part of the year, since photochemistry is a prerequisite for formation of, e.g. sulfuric acid in the gas phase.

Thus, the data was separated into two periods, one comprising data when the Arctic is dark (i.e. October–February), and one comprising data during the sunlit part of the year (i.e. March–September). The result is shown in Fig. 17 and 18, respectively. It becomes clear that the apparent number increase of smaller sized particles is much more pronounced during the summer months. It is also evident that this relative increase of small particles follows after an initial, significant, decrease of aerosols in the larger size classes (Fig. 17). When concentration of accumulation mode concentration is high (i.e. prior to substantial wet removal) the concentration of the finer fraction is very small and only increase after a large portion of the accumulation mode sized particles has been removed. It is also evident that during the dark half of the year, the apparent increase is missing although there is a substantial reduction of accumulation mode particle concentration (Fig. 18), suggesting that the increase is depending on the season, and thus possibly the rate of incoming solar radiation to support the photochemical reactions generating suitable precursor gases. It seems so that wet removal paves way for new particle formation via removal of larger sized particles and thus condensation sink, allowing high enough concentrations of precursor gases build up, supporting new particle formation. The rain would then act as a mechanism that facilitates a "shift of generation" with respect to the particle population. When the older bigger particles have been removed, a new aerosol starts to form, filling the gap created by the clouds and precipitation. It is also interesting to notice that these newly formed particles seem less accessible to removal by rain compared to the original, larger sized aerosols, as the sensitivity to increasing precipitation is less for higher integral values of accumulated amount of precipitation (mm_{tot}).

Consequently, it is suggested that clouds and rain and associated wet removal seem to be a key process in shaping the appearance of the Arctic aerosol. The effect of wet removal seem to be two-fold: it does not only include removal of larger size particles by

ACPD
12, 29967–30019, 2012

scavenging, but instead by removing the larger particles, rain events further establish conditions that favor new particle formation via nucleation.

Based on the findings presented in this study, a conceptually reasonable and qualitatively sound mechanistic explanation of the annual variation of aerosol properties may be proposed, whereby the key conditions to reach haze levels of particles include transport from areas with high emissions concurrent with sunlit transport conditions and low precipitation during transport.

4 Summary and conclusions

In this study we have presented a 10-yr data set of aerosol size distribution measurements collected at the Zeppelin station located on Svalbard. We have investigated the data based on seasonality and diurnal variability and provide transport climatology for the studied period. We have presented statistics for the size distribution properties, including estimates of log normal modal size distribution parameters on annual and monthly basis.

We have shown that the aerosol mass, surface and size number distribution properties are a strong function of season, and that this seasonality is repeated from year to year. During the haze period in late winter and spring, the aerosol is dominated by accumulation mode sized particles, and there seem to be an absence of contribution to particle number from local nucleation. Highest observed concentration of aerosol mass is observed when transport comes from of Russia and Central Europe. The dominating transport direction derived however, seem to be for all months except June–August, within an approximately 120° sector extending to Alaska in easterly direction and Northern Siberia in the westerly directions. Transport from land-based sources seems to be dominated by transport from Siberia, Eurasia and to some degree the European sub continent (which is in agreement with previous findings by Hirdman et al., 2010). Only a minor fraction of the 240 h trajectories extend down to East Asia and Central Asia. There is further a minimum influence of air mass transport over the Atlantic Ocean.

ACPD
12, 29967–30019, 2012

During the summer months June–August, a much larger fraction of air mass transport takes place over the Atlantic Ocean, and the summer season is characterized by higher fraction of smaller sized particles, which is suggested to have been formed locally.

We further show that the transport from the source regions into the Arctic during the Haze periods is characterized by low amounts of precipitation (on average 2–3 mm of rain during last 10 days), and that summer time is associated with highest amount of precipitation amount (on average 7–8 mm of rain during last 10 days). By investigating the relation between aerosol mass and calculated precipitation we demonstrate a strong link between observed mass and precipitation history, suggesting that wet removal largely control the properties of the aerosol size distribution observed in Svalbard. This is further supported by an analogous analysis of the size distribution properties and their relation to experienced amount of precipitation. During the winter period, wet removal gradually diminishes the accumulation mode particles and this decrease is most rapid when the amount of accumulated precipitation is comparably small. Performing the same analysis for the summer months demonstrated that although precipitation initially removes aerosol mass and number, wet removal also seem to facilitate conditions that favor new particle formation and growth. This was demonstrated as a gradual increase in nuclei-Aitken mode sized particles as the amount of precipitation increased further during the summer months. The fact that this was only observed during summer suggests that photochemistry plays a central role in formation of these small particles and that this formation of new particles only takes place when the balance between generation and removal of nucleating gases is favorable (i.e. source of pre-cursor gases, photochemical activity and low condensation sink).

Based on the findings, we can, at least qualitatively, describe the Arctic aerosol year based on the characteristics of land-based sources, sinks (mainly wet deposition) en route to Svalbard, and photochemical activity. Thus, during the Haze period, precipitation and wet removal is at a minimum, which result in effective transport of pollutants into the Arctic. Although the haze period is partly sunlit, the sink constituted by the large concentration of pre-existing aerosols hinders nucleation and growth. When entering

ACPD
12, 29967–30019, 2012

the summer, the source areas are shifted and the amount of precipitation increase which result in low mass and surface concentration. This low concentration of large sized particles and maximum photochemical activity leads to new particle formation, and the aerosol is dominated by a comparable large amount of small particles. During the end of the summer the intensity of sunlight decreases, and despite of low concentration of large particles, nucleation cease since the production of nucleating vapors is too slow. This state progresses during the rest of the year (October–February). The trajectories experience less and less precipitation during transport, which is reflected by increasing aerosol mass concentration. The combined effect of sources and sinks in terms of wet removal bring about a new haze event the following year and the cycle is repeated. In summary, precipitation seems to be a major factor, not only acting as a direct sink of particles, but also, wet removal provides the mechanism that allow for a generation shift of the aerosol population; situations with substantial wet removal provide a low enough condensation sink to allow for formation of new particle number to be formed via new particle formation events.

Although this mechanistic explanation seems to agree with the results presented in this study, a number of other mechanisms may play important roles. To a certain extent, our findings corroborate earlier mechanistic implications presented by, e.g. (Shaw, 1981; Quinn et al., 2007), especially regarding the characteristic transport conditions and absence of significant wet removal during the Arctic Haze period.

Acknowledgements. Funding for this study was provided through the Swedish Environmental Protection Agency (Naturvårdsverket, NV) as part of the Environmental monitoring program and from Swedish Research Council (Vetenskapsrådet, VR) within the framework of CLIMSLIP (CLimate IMpacts of Short-Lived Pollutants in the polar region).

ACPD
12, 29967–30019, 2012

References

Albrecht, B. A.: Aerosols, cloud microphysics, and fractional cloudiness, Science, 245, 1227–1230, doi:10.1126/science.245.4923.1227, 1989.

Behrenfeldt, U., Krejci, R., Strom, J., and Stohl, A.: Chemical properties of Arctic aerosol particles collected at the Zeppelin station during the aerosol transition period in May and June of 2004, Tellus B, 60, 405–415, doi:10.1111/j.1600-0889.2008.00349.x, 2008.

Beine, H. J., Argentini, S., Maurizi, A., Mastrantonio, G., and Viola, A.: The local wind field at Ny-Alesund and the Zeppelin mountain at Svalbard, Meteorol. Atmos. Phys., 78, 107–113, 2001.

Brock, C. A., Cozic, J., Bahreini, R., Froyd, K. D., Middlebrook, A. M., McComiskey, A., Brioude, J., Cooper, O. R., Stohl, A., Aikin, K. C., de Gouw, J. A., Fahey, D. W., Ferrare, R. A., Gao, R.-S., Gore, W., Holloway, J. S., Hübler, G., Jefferson, A., Lack, D. A., Lance, S., Moore, R. H., Murphy, D. M., Nenes, A., Novelli, P. C., Nowak, J. B., Ogren, J. A., Peischl, J., Pierce, R. B., Pilewskie, P., Quinn, P. K., Ryerson, T. B., Schmidt, K. S., Schwarz, J. P., Sodemann, H., Spackman, J. R., Stark, H., Thomson, D. S., Thornberry, T., Veres, P., Watts, L. A., Warneke, C., and Wollny, A. G.: Characteristics, sources, and transport of aerosols measured in spring 2008 during the aerosol, radiation, and cloud processes affecting Arctic Climate (ARCPAC) Project, Atmos. Chem. Phys., 11, 2423–2453, doi:10.5194/acp-11-2423-2011, 2011.

Buatmenard, P. and Duce, R. A.: Precipitation scavenging of aerosol-particles over remote marine regions, Nature, 321, 508–510, 1986.

Charlson, R. J., Schwartz, S. E., Hales, J. M., Cess, R. D., Coakley, J. A., Hansen, J. E., and Hofmann, D. J.: Climate forcing by anthropogenic aerosols, Science, 255, 423–430, doi:10.1126/science.255.5043.423, 1992.

Clarke, A. D. and Noone, K. J.: Soot in the Arctic – a cause for perturbations in radiative transfer, Atmos. Environ., 19, 2045–2053, doi:10.1016/0004-6981(85)90113-1, 1985.

Dal Maso, M., Kulmala, M., Riipinen, I., Wagner, R., Hussein, T., Aalto, P. P., and Lehtinen, K. E. J.: Formation and growth of fresh atmospheric aerosols: eight years of aerosol size distribution data from SMEAR II, Hyytiala, Finland, Boreal Environ. Res., 10, 323–336, 2005.

Dal Maso, M., Sogacheva, L., Aalto, P. P., Riipinen, I., Komppula, M., Tunved, P., Korhonen, L., Suur-Uski, V., Hirsikko, A., Kurten, T., Kerminen, V. M., Lihavainen, H., Viisanen, Y., Hans-

ACPD
12, 29967–30019, 2012

son, H. C., and Kulmala, M.: Aerosol size distribution measurements at four nordic field stations: identification, analysis and trajectory analysis of new particle formation bursts, Tellus B, 59, 350–361, doi:10.1111/j.1600-0889.2007.00267.x, 2007.

Engström, A. and Magnusson, L.: Estimating trajectory uncertainties due to flow dependent errors in the atmospheric analysis, Atmos. Chem. Phys., 9, 8857–8867, doi:10.5194/acp-9-8857-2009, 2009.

Engvall, A. C., Krejci, R., Strom, J., Minikin, A., Treffeisen, R., Stohl, A., and Herber, A.: In-situ airborne observations of the microphysical properties of the Arctic tropospheric aerosol during late spring and summer, Tellus B, 60, 392–404, doi:10.1111/j.1600-0889.2008.00348.x, 2008a.

Engvall, A.-C., Krejci, R., Ström, J., Treffeisen, R., Scheele, R., Hermansen, O., and Paatero, J.: Changes in aerosol properties during spring-summer period in the Arctic troposphere, Atmos. Chem. Phys., 8, 445–462, doi:10.5194/acp-8-445-2008, 2008b.

Fisher, J. A., Jacob, D. J., Purdy, M. T., Kopacz, M., Le Sager, P., Carouge, C., Holmes, C. D., Yantosca, R. M., Batchelor, R. L., Strong, K., Diskin, G. S., Fuelberg, H. E., Holloway, J. S., Hyer, E. J., McMillan, W. W., Warner, J., Streets, D. G., Zhang, Q., Wang, Y., and Wu, S.: Source attribution and interannual variability of Arctic pollution in spring constrained by aircraft (ARCTAS, ARCPAC) and satellite (AIRS) observations of carbon monoxide, Atmos. Chem. Phys., 10, 977–996, doi:10.5194/acp-10-977-2010, 2010.

Flanner, M. G., Zender, C. S., Randerson, J. T., and Rasch, P. J.: Present-day climate forcing and response from black carbon in snow, J. Geophys. Res.-Atmos., 112, D11202, doi:10.1029/2006jd008003, 2007.

Garrett, T. J., Radke, L. F., and Hobbs, P. V.: Aerosol effects on cloud emissivity and surface longwave heating in the arctic, J. Atmos. Sci., 59, 769–778, doi:10.1175/1520-0469(2002)059<0769:aeocea>2.0.co;2, 2002.

Guibert, S., Snider, J. R., and Brenguier, J. L.: Aerosol activation in marine stratocumulus clouds: 1. Measurement validation for a closure study, J. Geophys. Res.-Atmos., 108, 8628, doi:10.1029/2002jd002678, 2003.

Hansen, J. and Nazarenko, L.: Soot climate forcing via snow and ice albedos, P. Natl. Acad. Sci. USA, 101, 423–428, doi:10.1073/pnas.2237157100, 2004.

Hegg, D. A., Ferek, R. J., and Hobbs, P. V.: Cloud condensation nuclei over the Arctic-Ocean in early spring, J. Appl. Meteorol., 34, 2076–2082, 1995.

ACPD
12, 29967–30019, 2012

Heintzenberg, J., Hansson, H. C., and Lannefors, H.: The chemical composition of arctic haze at Ny-Alesund, Spitsbergen, Tellus, 33, 162–171, 1981.
Hirdman, D., Sodemann, H., Eckhardt, S., Burkhart, J. F., Jefferson, A., Mefford, T., Quinn, P. K., Sharma, S., Ström, J., and Stohl, A.: Source identification of short-lived air pollutants in the Arctic using statistical analysis of measurement data and particle dispersion model output, Atmos. Chem. Phys., 10, 669–693, doi:10.5194/acp-10-669-2010, 2010.
Hoppel, W. A. and Frick, G. M.: Submicron aerosol size distributions measured over the tropical and Southern Pacific, Atmos. Environ. A-Gen., 24, 645–659, doi:10.1016/0960-1686(90)90020-n, 1990.
Hu, R. M., Blanchet, J. P., and Girard, E.: Evaluation of the direct and indirect radiative and climate effects of aerosols over the Western Arctic, J. Geophys. Res.-Atmos., 110, D11213, doi:10.1029/2004jd005043, 2005.
Hudson, S. R.: Estimating the global radiative impact of the sea ice-albedo feedback in the Arctic, J. Geophys. Res.-Atmos., 116, D16102, doi:10.1029/2011jd015804, 2011.
Iversen, T. and Joranger, E.: Arctic air pollution and large scale atmospheric flows, Atmos. Environ., 19, 2099–2108, doi:10.1016/0004-6981(85)90117-9, 1985.
Iziomon, M. G., Lohmann, U., and Quinn, P. K.: Summertime pollution events in the Arctic and potential implications, J. Geophys. Res.-Atmos., 111, D12206, doi:10.1029/2005jd006223, 2006.
Jaeschke, W., Beltz, N., Dierssen, J. P., Haunold, W., Krischke, U., Reinecke, A., Salkowski, T., and VonTrumbach, J.: Measurements on the distribution of trace substances in the Arctic troposphere, Atmos. Res., 44, 199–221, 1997.
Jaeschke, W., Salkowski, T., Dierssen, J. P., Trumbach, J. V., Krischke, U., and Gunther, A.: Measurements of trace substances in the Arctic troposphere as potential precursors and constituents of Arctic haze, J. Atmos. Chem., 34, 291–319, 1999.
Jokinen, V. and Makela, J. M.: Closed-loop arrangement with critical orifice for DMA sheath excess flow system, J. Aerosol. Sci., 28, 643–648, 1997.
Khosrawi, F., Ström, J., Minikin, A., and Krejci, R.: Particle formation in the Arctic free troposphere during the ASTAR 2004 campaign: a case study on the influence of vertical motion on the binary homogeneous nucleation of H_2SO_4/H_2O, Atmos. Chem. Phys., 10, 1105–1120, doi:10.5194/acp-10-1105-2010, 2010.
Knutson, E. O. and Whitby, K. T.: Anomalous unipolar diffusion charging of plystyrene aerosols, J. Colloid Interf. Sci., 53, 493–495, doi:10.1016/0021-9797(75)90067-3, 1975.

ACPD
12, 29967–30019, 2012

Koponen, I. K., Virkkula, A., Hillamo, R., Kerminen, V. M., and Kulmala, M.: Number size distributions and concentrations of the continental summer aerosols in Queen Maud Land, Antarctica, J. Geophys. Res., 108, 4587, doi:10.1029/2003jd003614, 2003.
Kulmala, M. and Kerminen, V. M.: On the formation and growth of atmospheric nanoparticles, Atmos. Res., 90, 132–150, doi:10.1016/j.atmosres.2008.01.005, 2008.
Lubin, D. and Vogelmann, A. M.: Observational quantification of a total aerosol indirect effect in the Arctic, Tellus B, 62, 181–189, 2010.
O'Neill, N. T., Pancrati, O., Baibakov, K., Eloranta, E., Batchelor, R. L., Freemantle, J., McArthur, L. J. B., Strong, K., and Lindenmaier, R.: Occurrence of weak, sub-micron, tropospheric aerosol events at high Arctic latitudes, Geophys. Res. Lett., 35, L14814, doi:10.1029/2008gl033733, 2008.
Polissar, A. V., Hopke, P. K., and Paatero, P.: Atmospheric aerosol over Alaska – 2. Elemental composition and sources, J. Geophys. Res.-Atmos., 103, 19045–19057, doi:10.1029/98jd01212, 1998.
Polissar, A. V., Hopke, P. K., and Harris, J. M.: Source regions for atmospheric aerosol measured at Barrow, Alaska, Environ. Sci. Technol., 35, 4214–4226, doi:10.1021/es0107529, 2001.
Quinn, P. K., Shaw, G., Andrews, E., Dutton, E. G., Ruoho-Airola, T., and Gong, S. L.: Arctic haze: current trends and knowledge gaps, Tellus B, 59, 99–114, doi:10.1111/j.1600-0889.2006.00238.x, 2007.
Robock, A.: Ice and snow feedbacks and the latitudinal and seasonal distribution of climate sensitivity, J. Atmos. Sci., 40, 986–997, 1983.
Rosen, H., Novakov, T., and Bodhaine, B. A.: Soot in the Arctic, Atmos. Environ., 15, 1371–1374, doi:10.1016/0004-6981(81)90343-7, 1981.
Schmale, J., Schneider, J., Ancellet, G., Quennehen, B., Stohl, A., Sodemann, H., Burkhart, J. F., Hamburger, T., Arnold, S. R., Schwarzenboeck, A., Borrmann, S., and Law, K. S.: Source identification and airborne chemical characterisation of aerosol pollution from long-range transport over Greenland during POLARCAT summer campaign 2008, Atmos. Chem. Phys., 11, 10097–10123, doi:10.5194/acp-11-10097-2011, 2011.
Serreze, M. C., Holland, M. M., and Stroeve, J.: Perspectives on the Arctic's shrinking sea-ice cover, Science, 315, 1533–1536, 2007.
Sharma, S., Chan, E., Ishizawa, M., Toom-Sauntry, D., Gong, S. L., Li, S. M., Tarasick, D. W., Leaitch, W. R., Norman, A., Quinn, P. K., Bates, T. S., Levasseur, M., Barrie, L. A., and

ACPD
12, 29967–30019, 2012

Maenhaut, W.: Influence of transport and ocean ice extent on biogenic aerosol sulfur in the Arctic atmosphere, J. Geophys. Res.-Atmos., 117, 12, doi:10.1029/2011jd017074, 2012.
Shaw, G. E.: Eddy diffusion transport of Arctic pollution from the Mid-Latitudes, Atmos. Environ., 15, 1483–1490, doi:10.1016/0004-6981(81)90356-5, 1981.
Shaw, G. E.: Production of condensation nuclei in clean air by nycleation of H_2SO_4, Atmos. Environ., 23, 2841–2846, doi:10.1016/0004-6981(89)90564-7, 1989.
Shaw, G. E.: The arctic haze phenomenon, B. Am. Meteorol. Soc., 76, 2403–2413, 1995.
Shindell, D. and Faluvegi, G.: Climate response to regional radiative forcing during the twentieth century, Nat. Geosci., 2, 294–300, doi:10.1038/ngeo473, 2009.
Shupe, M. D. and Intrieri, J. M.: Cloud radiative forcing of the Arctic surface: the influence of cloud properties, surface albedo, and solar zenith angle, J. Climate, 17, 616–628, doi:10.1175/1520-0442(2004)017<0616:crfota>2.0.co;2, 2004.
Snider, J. R., Guibert, S., Brenguier, J. L., and Putaud, J. P.: Aerosol activation in marine stratocumulus clouds: 2. Kohler and parcel theory closure studies, J. Geophys. Res.-Atmos., 108, 8629, doi:10.1029/2002jd002692, 2003.
Stohl, A.: Characteristics of atmospheric transport into the Arctic troposphere, J. Geophys. Res.-Atmos., 111, D11306, doi:10.1029/2005jd006888, 2006.
Stohl, A., Berg, T., Burkhart, J. F., Fjaeraa, A. M., Forster, C., Herber, A., Hov, Ø., Lunder, C., McMillan, W. W., Oltmans, S., Shiobara, M., Simpson, D., Solberg, S., Stebel, K., Ström, J., Tørseth, K., Treffeisen, R., Virkkunen, K., and Yttri, K. E.: Arctic smoke – record high air pollution levels in the European Arctic due to agricultural fires in Eastern Europe in spring 2006, Atmos. Chem. Phys., 7, 511–534, doi:10.5194/acp-7-511-2007, 2007.
Strom, J., Umegard, J., Torseth, K., Tunved, P., Hansson, H. C., Holmen, K., Wismann, V., Herber, A., and Konig-Langlo, G.: One year of particle size distribution and aerosol chemical composition measurements at the Zeppelin Station, Svalbard, March 2000–March 2001, Phys. Chem. Earth., 28, 1181–1190, doi:10.1016/j.pce.2003.08.058, 2003.
Strom, J., Engvall, A. C., Delbart, F., Krejci, R., and Treffeisen, R.: On small particles in the Arctic summer boundary layer: observations at two different heights near Ny-Alesund, Svalbard, Tellus B, 61, 473–482, doi:10.1111/j.1600-0889.2008.00412.x, 2009.
Textor, C., Schulz, M., Guibert, S., Kinne, S., Balkanski, Y., Bauer, S., Berntsen, T., Berglen, T., Boucher, O., Chin, M., Dentener, F., Diehl, T., Easter, R., Feichter, H., Fillmore, D., Ghan, S., Ginoux, P., Gong, S., Grini, A., Hendricks, J., Horowitz, L., Huang, P., Isaksen, I., Iversen, I., Kloster, S., Koch, D., Kirkevåg, A., Kristjansson, J. E., Krol, M., Lauer, A., Lamarque, J. F.,

ACPD
12, 29967–30019, 2012

Liu, X., Montanaro, V., Myhre, G., Penner, J., Pitari, G., Reddy, S., Seland, Ø., Stier, P., Takemura, T., and Tie, X.: Analysis and quantification of the diversities of aerosol life cycles within AeroCom, Atmos. Chem. Phys., 6, 1777–1813, doi:10.5194/acp-6-1777-2006, 2006.

Tunved, P., Ström, J., and Hansson, H.-C.: An investigation of processes controlling the evolution of the boundary layer aerosol size distribution properties at the Swedish background station Aspvreten, Atmos. Chem. Phys., 4, 2581–2592, doi:10.5194/acp-4-2581-2004, 2004.

Twomey, S.: Influence of pollution on shortwave albedo of clouds, J. Atmos. Sci., 34, 1149–1152, doi:10.1175/1520-0469(1977)034<1149:tiopot>2.0.co;2, 1977.

Van Dingenen, R., Raes, F., Putaud, J. P., Baltensperger, U., Charron, A., Facchini, M. C., Decesari, S., Fuzzi, S., Gehrig, R., Hansson, H. C., Harrison, R. M., Huglin, C., Jones, A. M., Laj, P., Lorbeer, G., Maenhaut, W., Palmgren, F., Querol, X., Rodriguez, S., Schneider, J., ten Brink, H., Tunved, P., Torseth, K., Wehner, B., Weingartner, E., Wiedensohler, A., and Wahlin, P.: A European aerosol phenomenology-1: physical characteristics of particulate matter at kerbside, urban, rural and background sites in Europe, Atmos. Environ., 38, 2561–2577, doi:10.1016/j.atmosenv.2004.01.040, 2004.

Wang, M. Y. and Overland, J. E.: A sea ice free summer Arctic within 30 years?, Geophys. Res. Lett., 36, L18501, doi:10.1029/2012gl052868, 2009.

Warneke, C., Bahreini, R., Brioude, J., Brock, C. A., de Gouw, J. A., Fahey, D. W., Froyd, K. D., Holloway, J. S., Middlebrook, A., Miller, L., Montzka, S., Murphy, D. M., Peischl, J., Ryerson, T. B., Schwarz, J. P., Spackman, J. R., and Veres, P.: Biomass burning in Siberia and Kazakhstan as an important source for haze over the Alaskan Arctic in April 2008, Geophys. Res. Lett., 36, L02813, doi:10.1029/2008gl036194, 2009.

Weber, R. J., Orsini, D., Wang, B., Scheuer, E., Talbot, R. W., Dibb, J. E., Seid, G. K., DeBell, L., Mauldin, R. L., Kosciuch, E., Cantrell, C., and Eisele, F.: Investigations into free tropospheric new particle formation in the Central Canadian arctic during the winter/spring transition as part of TOPSE, J. Geophys. Res.-Atmos., 108, 8357, doi:10.1029/2002jd002239, 2003.

ACPD
12, 29967–30019, 2012

Table 1. Median modal properties of the aerosol number size distribution as observed at Mt. Zeppelin March 2000–March 2010. 25th–75th percentile range within brackets, mean values within square brackets. Given are the median of modal number concentration (N, cm^{-3}), modal geometrical standard deviation (GSD) and modal geometrical mean diameter (D_g, µm).

	N (cm^{-3})	GSD	D_g (µm)
Mode 1	13 [40] (5–36)	1.43 [1.55] (1.29–1.69)	0.0315 [0.0311] (0.0248–0.0386)
Mode 2	24 [54] (8–61)	1.50 [1.60] (1.31–1.80)	0.0841 [0.084] (0.0549–0.1120)
Mode 3	37 [82] (10–93)	1.50 [1.55] (1.39–1.62)	0.1555 [0.177] (0.1316–0.1895)

ACPD
12, 29967–30019, 2012

Table 2. Modal parameters and their corresponding 25th–75th percentile ranges for the period March 2000–December 2010. The lognormal fitting is based on daily average data for the selected time period. Given are the median of modal number concentration (N, cm^{-3}), modal geometrical standard deviation (GSD) and modal geometrical mean diameter (D_g, µm) for modes 1–3.

	$N1$ (cm^{-3})	GSD 1	$D_{g,1}$ (µm)	$N2$ (cm^{-3})	GSD 2	$D_{g,2}$ (µm)	$N3$ (cm^{-3})	GSD 3	$D_{g,3}$ (µm)
Jan	9 (4–17)	1.54 (1.36–1.83)	0.0319 (0.024–0.04)	13 (3–26)	1.42 (1.22–1.83)	0.1043 (0.069–0.122)	40 (16–82)	1.45 (1.37–1.61)	0.177 (0.15–0.224)
Feb	10 (4–28)	1.57 (1.38–1.85)	0.0312 (0.024–0.039)	25 (9–55)	1.49 (1.28–1.79)	0.1095 (0.081–0.13)	53 (23–102)	1.44 (1.36–1.56)	0.1851 (0.16–0.227)
Mar	10 (5–21)	1.44 (1.31–1.67)	0.0365 (0.029–0.04)	26 (9–55)	1.58 (1.28–1.91)	0.0977 (0.066–0.124)	102 (41–172)	1.48 (1.41–1.57)	0.1712 (0.149–0.198)
Apr	13 (6–29)	1.4 (1.3–1.59)	0.0359 (0.028–0.04)	26 (9–67)	1.61 (1.29–1.9)	0.0962 (0.06–0.128)	119 (54–188)	1.51 (1.45–1.58)	0.1632 (0.148–0.186)
May	21 (6–54)	1.37 (1.26–1.54)	0.0316 (0.025–0.039)	32 (11–67)	1.55 (1.3–1.89)	0.0682 (0.048–0.114)	75 (32–125)	1.57 (1.49–1.63)	0.1558 (0.139–0.178)
Jun	36 (10–92)	1.36 (1.25–1.57)	0.0297 (0.025–0.035)	44 (16–101)	1.49 (1.36–1.74)	0.0619 (0.048–0.091)	34 (11–80)	1.53 (1.4–1.63)	0.1407 (0.13–0.168)
Jul	40 (11–111)	1.44 (1.27–1.79)	0.0308 (0.024–0.037)	64 (25–135)	1.49 (1.35–1.71)	0.0558 (0.048–0.076)	31 (7–77)	1.5 (1.39–1.6)	0.1312 (0.13–0.158)
Aug	34 (9–71)	1.38 (1.26–1.66)	0.0306 (0.025–0.036)	45 (18–99)	1.48 (1.36–1.67)	0.0606 (0.046–0.085)	16 (3–49)	1.47 (1.36–1.61)	0.13 (0.13–0.152)
Sep	14 (4–30)	1.34 (1.27–1.54)	0.0291 (0.023–0.036)	24 (8–47)	1.53 (1.41–1.76)	0.0812 (0.055–0.101)	9 (2–25)	1.49 (1.32–1.65)	0.1409 (0.13–0.186)
Oct	6 (2–11)	1.48 (1.34–1.75)	0.0296 (0.024–0.037)	10 (4–26)	1.53 (1.37–1.84)	0.0953 (0.072–0.112)	12 (2–33)	1.53 (1.42–1.66)	0.1495 (0.13–0.183)
Nov	7 (4–12)	1.48 (1.35–1.65)	0.0316 (0.027–0.038)	9 (4–22)	1.51 (1.3–1.89)	0.0972 (0.067–0.117)	26 (6–47)	1.5 (1.39–1.62)	0.1612 (0.141–0.198)
Dec	10 (4–22)	1.6 (1.41–1.95)	0.0299 (0.023–0.037)	12 (4–25)	1.38 (1.25–1.79)	0.1017 (0.068–0.126)	36 (16–91)	1.5 (1.4–1.68)	0.1707 (0.144–0.203)

ACPD
12, 29967–30019, 2012

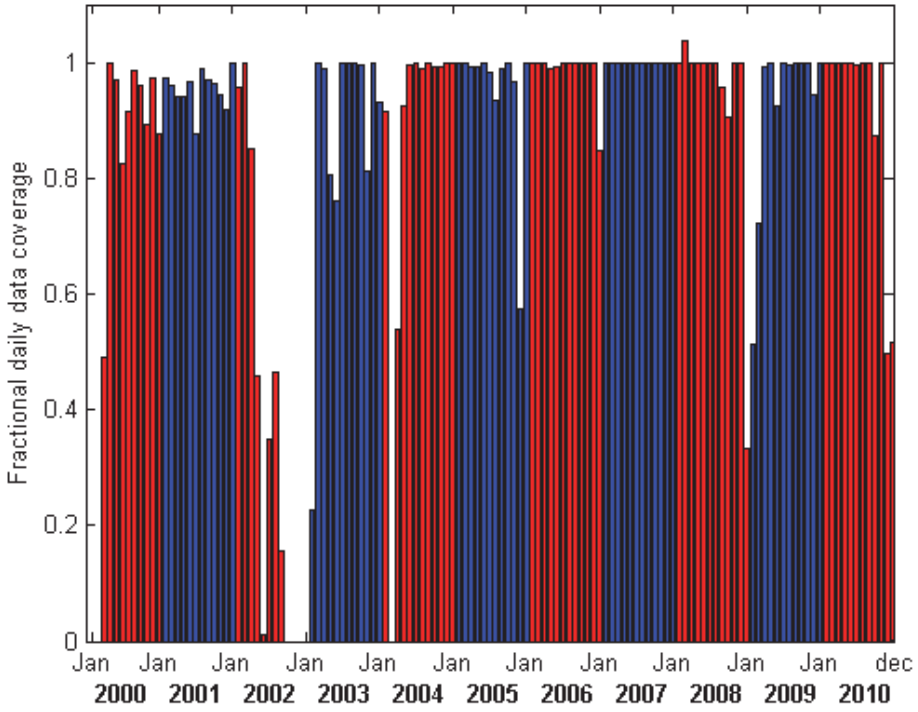

Fig. 1. Data coverage as fraction per month for the investigated period March 2000–March 2010. Data is shown as percent of daily averages.

ACPD
12, 29967–30019, 2012

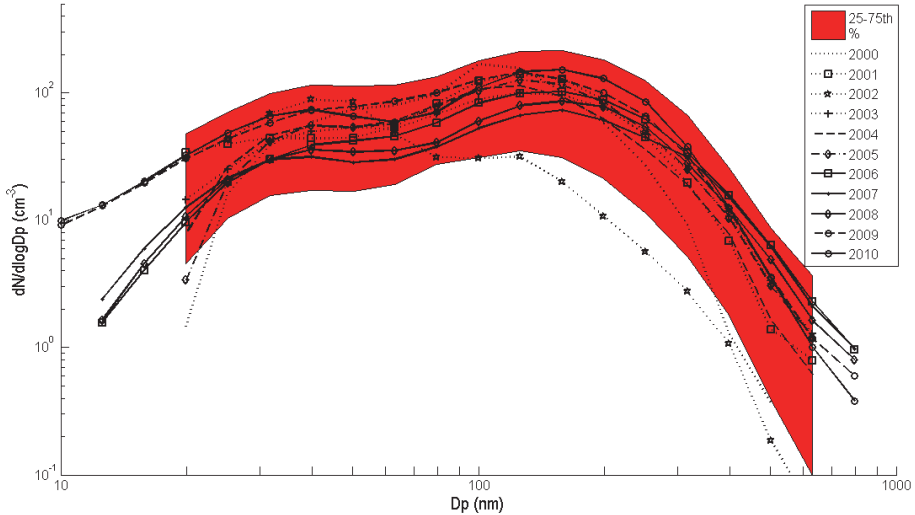

Fig. 2. Percentile range of aerosol number size distributions collected during 2000–2010 (red surface) and corresponding annual median aerosol number size distributions (black lines); pre-2006 data as dashed lines and post 2006 data as solid lines. Units in dN/dlogD_p, cm^{-3}.

ACPD
12, 29967–30019, 2012

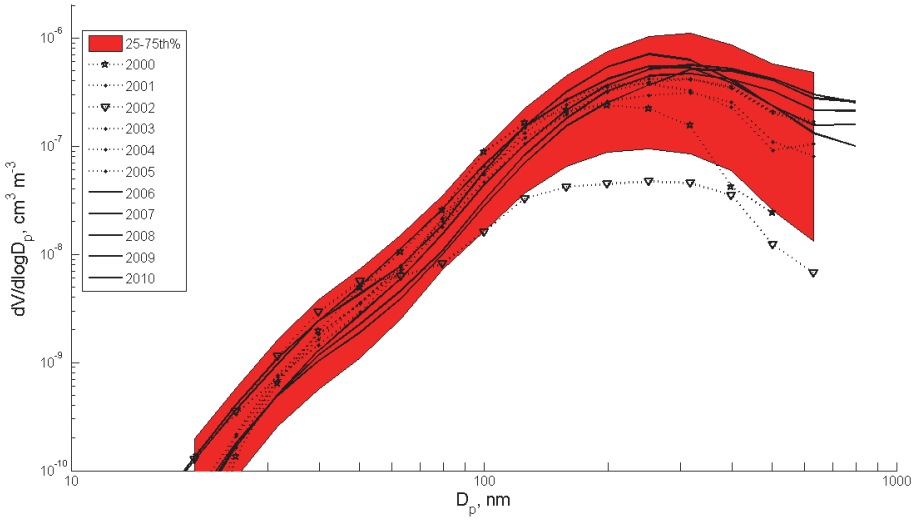

Fig. 3. Percentile range of aerosol volume size distributions collected during 2000–2010 (red surface) and corresponding annual median aerosol number size distributions (black lines); pre-2006 data as dashed lines and post 2006 data as solid lines. $dV/d\log D_p$, $cm^3\,m^{-3}$.

ACPD
12, 29967–30019, 2012

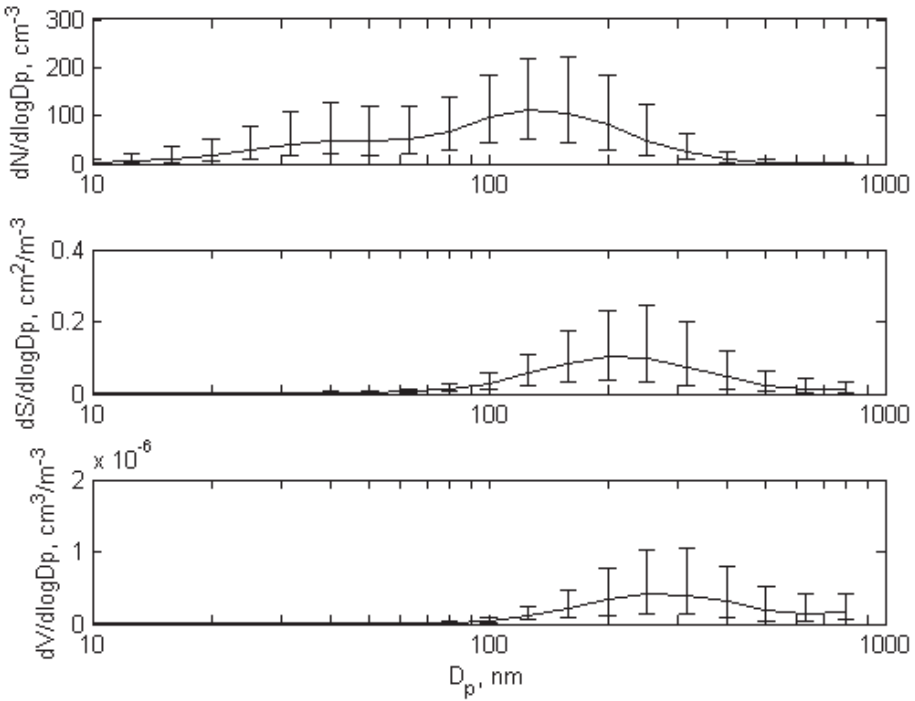

Fig. 4. Aerosol size distribution properties for the period March 2000–March 2010 and 25th–75th percentile ranges indicated. Top panel: Median aerosol number size distribution. Units in cm^{-3}. Middle panel: Median aerosol volume size distribution. Units in $cm^3\,m^{-3}$. Bottom panel: Median aerosol surface distribution. Units in $cm^2\,m^{-3}$.

ACPD
12, 29967–30019, 2012

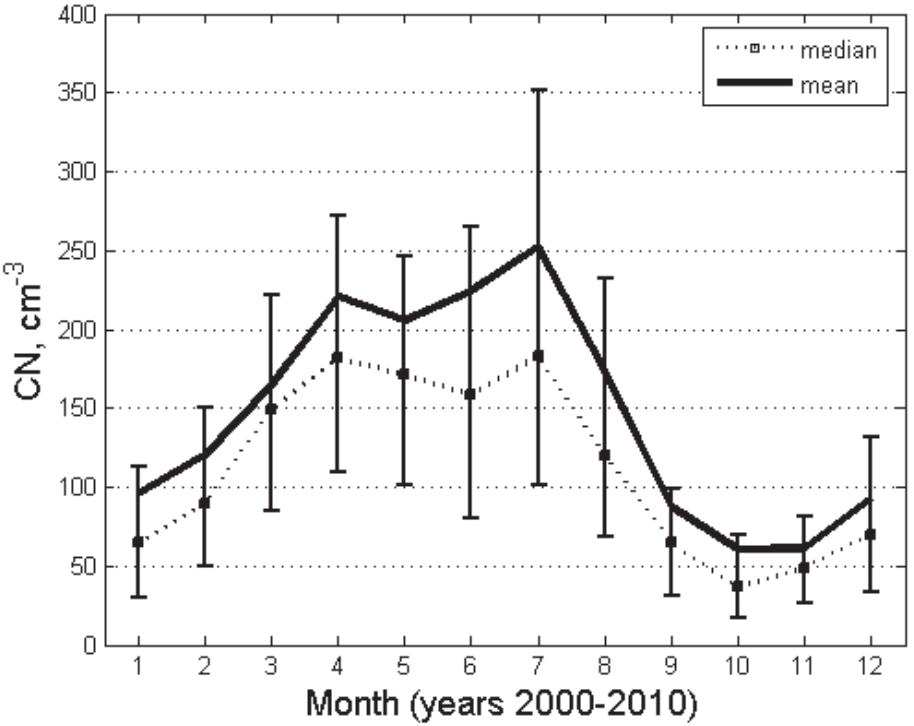

Fig. 5. Annual average variation of median and mean integrated number concentration per month March 2000–March 2010. 25th–75th percentile ranges indicated by vertical "error bars".

ACPD
12, 29967–30019, 2012

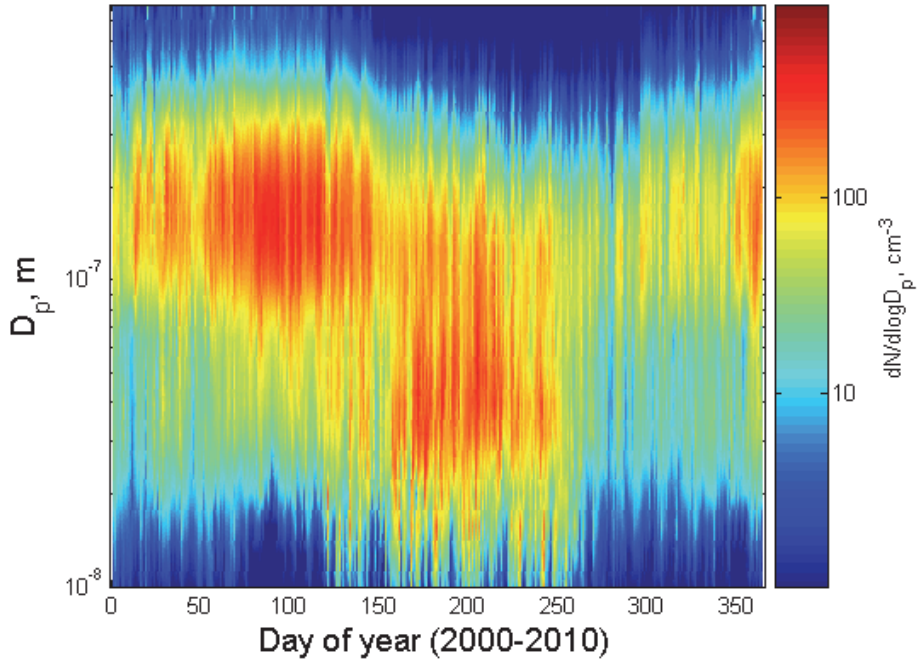

Fig. 6. Spectral plot of daily average aerosol number size distributions March 2000–December 2010. Units on x-axis as day of year.

ACPD
12, 29967–30019, 2012

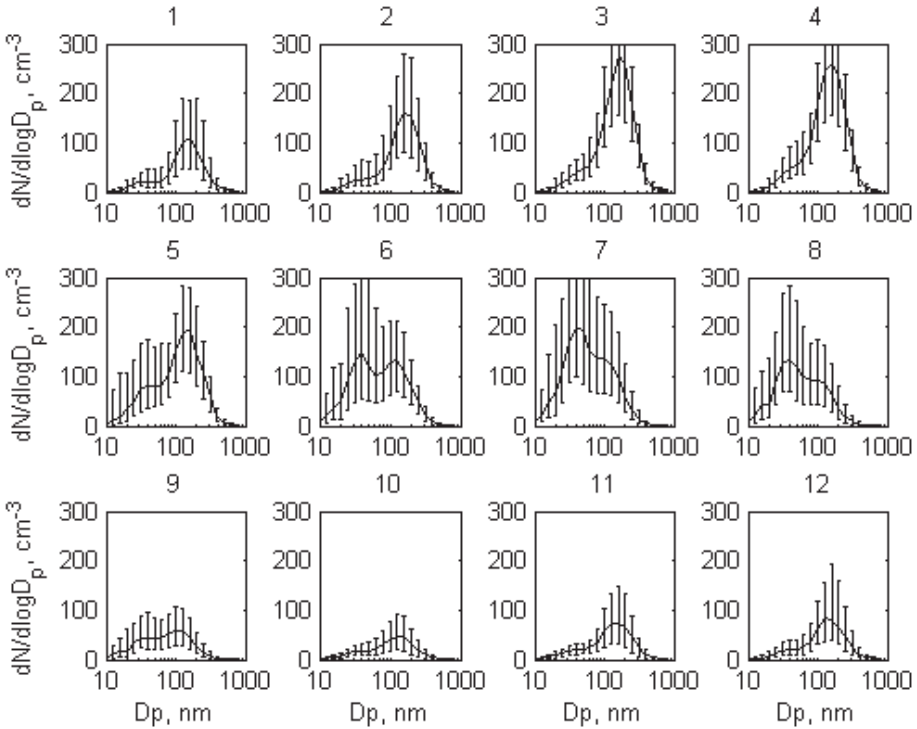

Fig. 7. Monthly median size distributions for years March 2000–March 2010. 25th–75th percentile ranges indicated by errorbars. Corresponding lognormal fitting parameters are shown in Table 2.

ACPD
12, 29967–30019, 2012

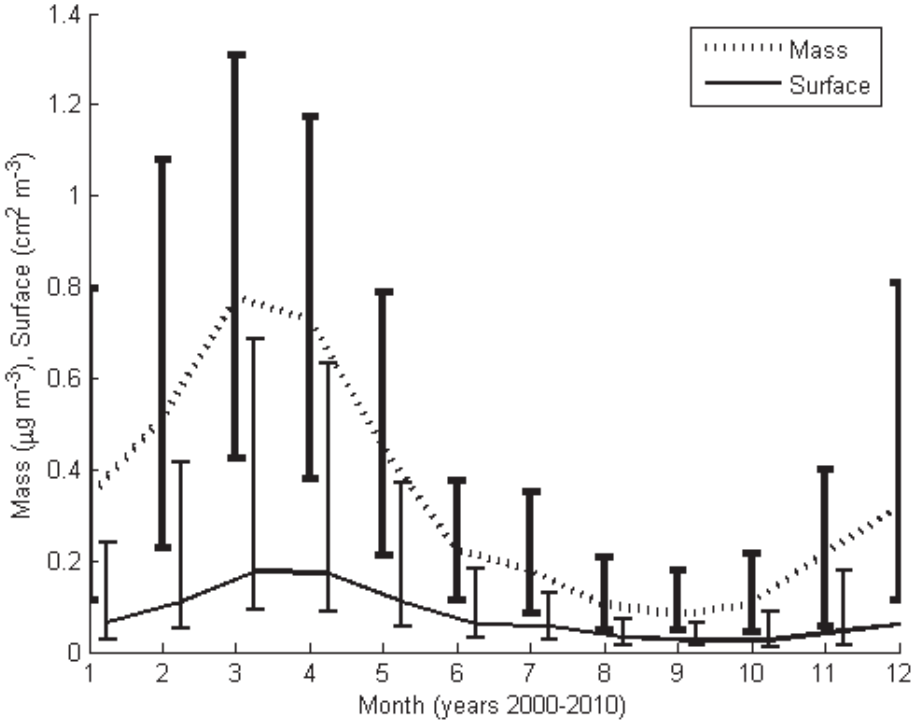

Fig. 8. Annual average variation of integrated surface and mass March 2000–March 2010. Mass data calculated from aerosol number size distribution assuming a density of $\rho = 1\,\mathrm{g\,cm^{-3}}$. 25th–75th percentile ranges indicated by errorbars.

ACPD
12, 29967–30019, 2012

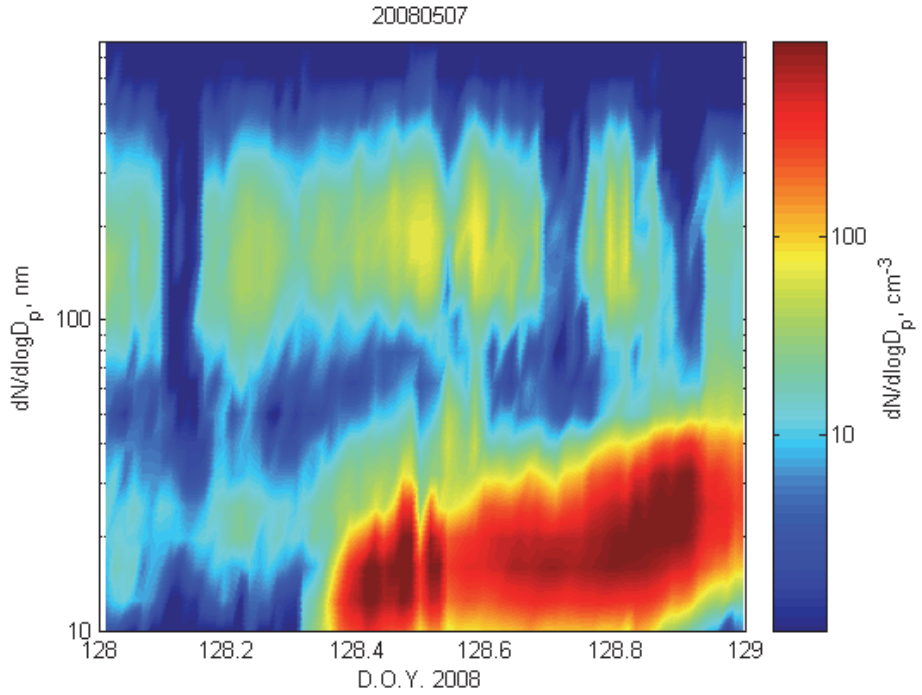

Fig. 9. Example of an Arctic nucleation event as observed 7 May 2008. dN/dlogD_p (cm^{-3}) versus decimal day of year (D.O.Y.).

ACPD
12, 29967–30019, 2012

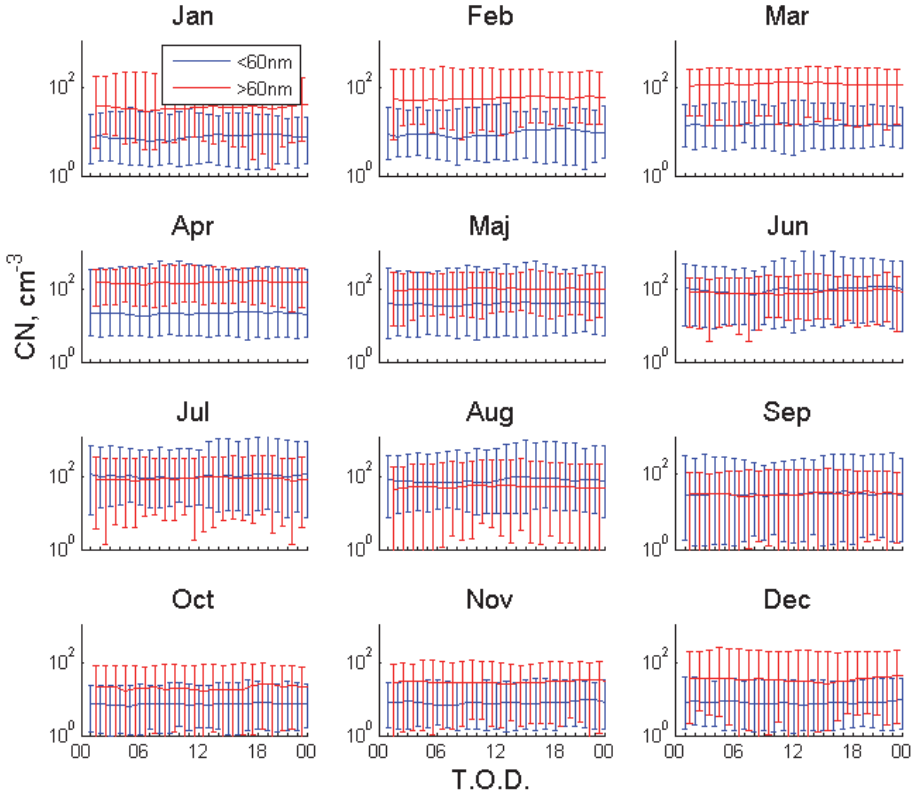

Fig. 10. Monthly (month 1–12) diurnal variation of number concentration $D_p < 60$ nm and $D_p > 60$ nm. 5th–95th percentile ranges indicated by errorbars. March 2000–March 2010. T.O.D. represents "Time of Day".

ACPD
12, 29967–30019, 2012

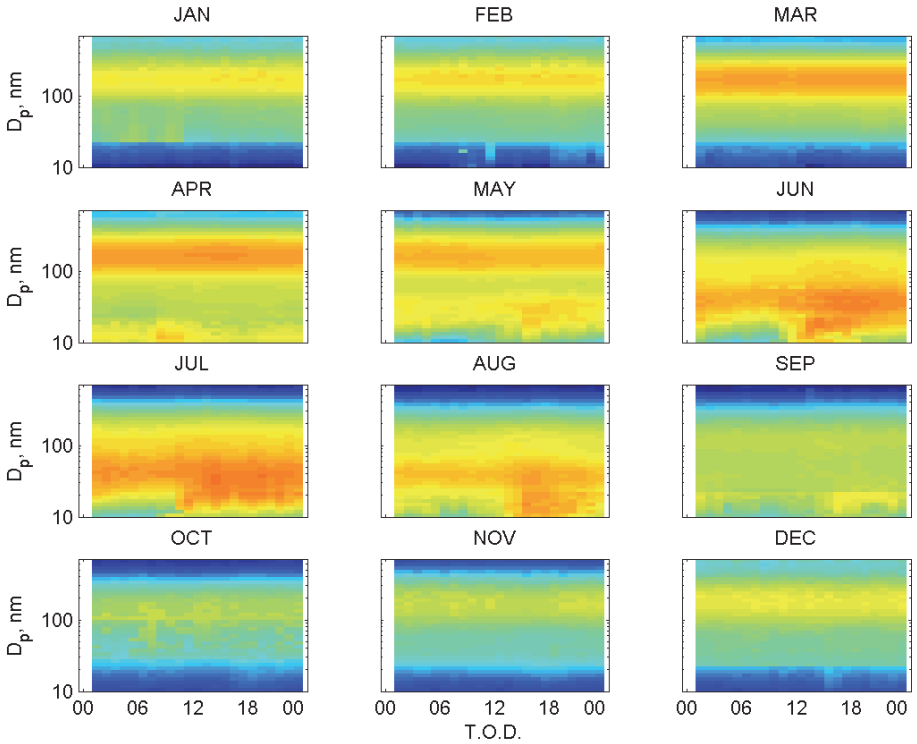

Fig. 11. Monthly diurnal variation of the 95th percentile of the aerosol number size distribution. T.O.D. represents "Time of Day".

ACPD
12, 29967–30019, 2012

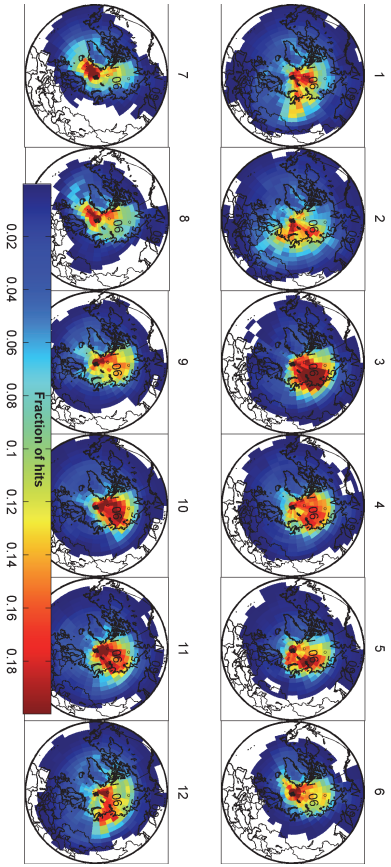

Fig. 12. Monthly, relative source distribution of trajectories arrving to Mt Zeppelin. Map display the average possibility that any single trajectory have resider above a certain grid. This is calculated by dividing the number of times each grid have been passed by a trajectory and dividing this number by the total number of trajectories arrviing to the receptor during that month. Data represents years 2000–2010.

ACPD
12, 29967–30019, 2012

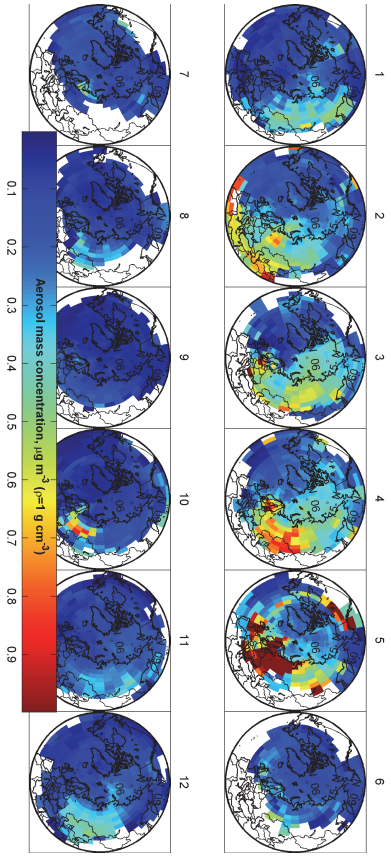

Fig. 13. Monthly maps showing the average concentration of submicron mass observed at Svalbard after crossing different source areas. Data represents years 2000–2010 (see text for details).

ACPD
12, 29967–30019, 2012

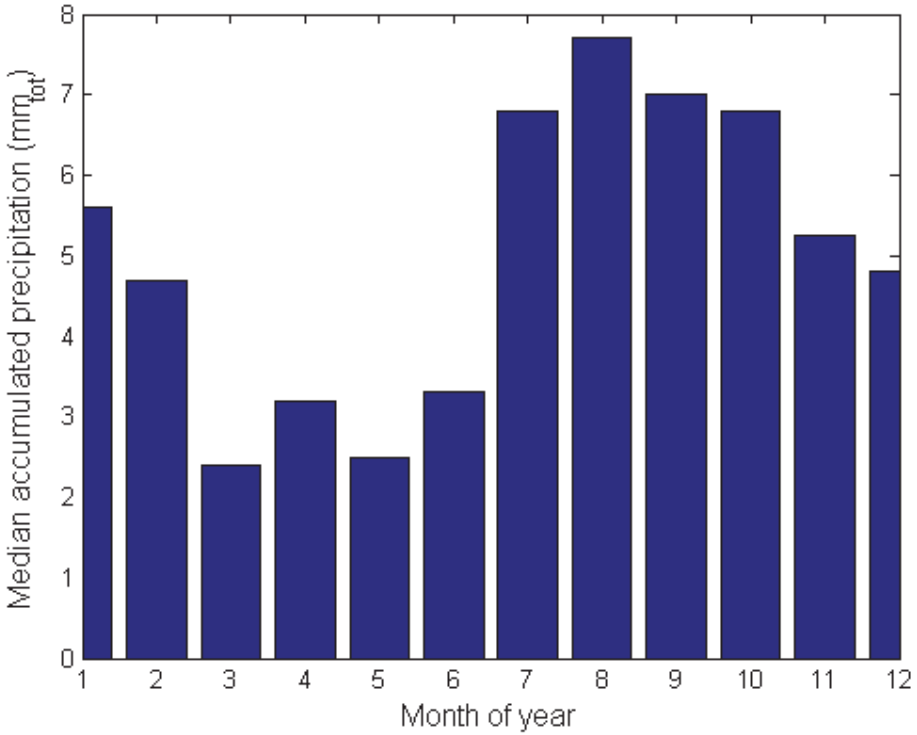

Fig. 14. Monthly median of accumulated precipitation experience by trajectories arriving to Svalbard during the period 2000–2010.

ACPD
12, 29967–30019, 2012

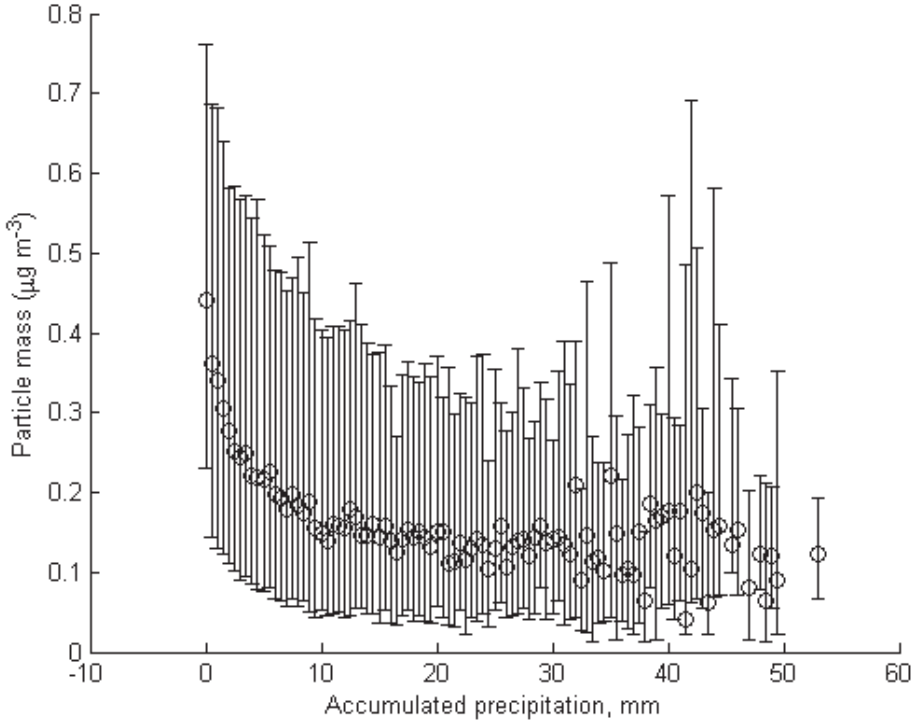

Fig. 15. Submicron aerosol mass evolution (10–630 nm; $\rho = 1\,\mathrm{g\,cm^{-3}}$) as a function of accumulated precipitation along the trajectories. Data is shown as 25th–75th percentile ranges per bin (solid lines) and median (circles). The figure includes all data collected between 2000 and 2010.

ACPD
12, 29967–30019, 2012

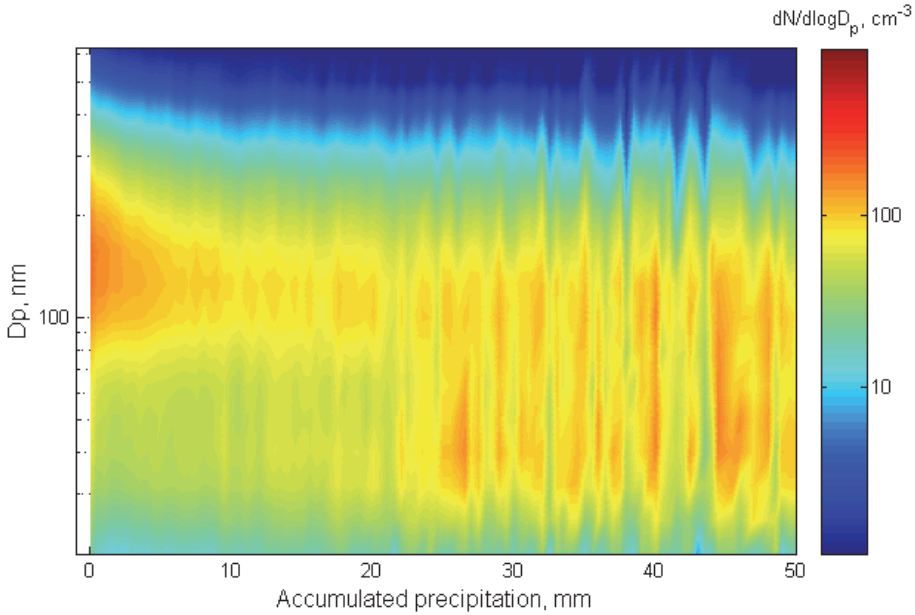

Fig. 16. Evolution of aerosol number size distribution as a function of accumulated precipitation (mm_{tot}) along 240 h trajectories. Data is shown binned over a step size of 0.5 mm_{tot} and the corresponding size distributions over this ranges of precipitation is presented as median values.

ACPD
12, 29967–30019, 2012

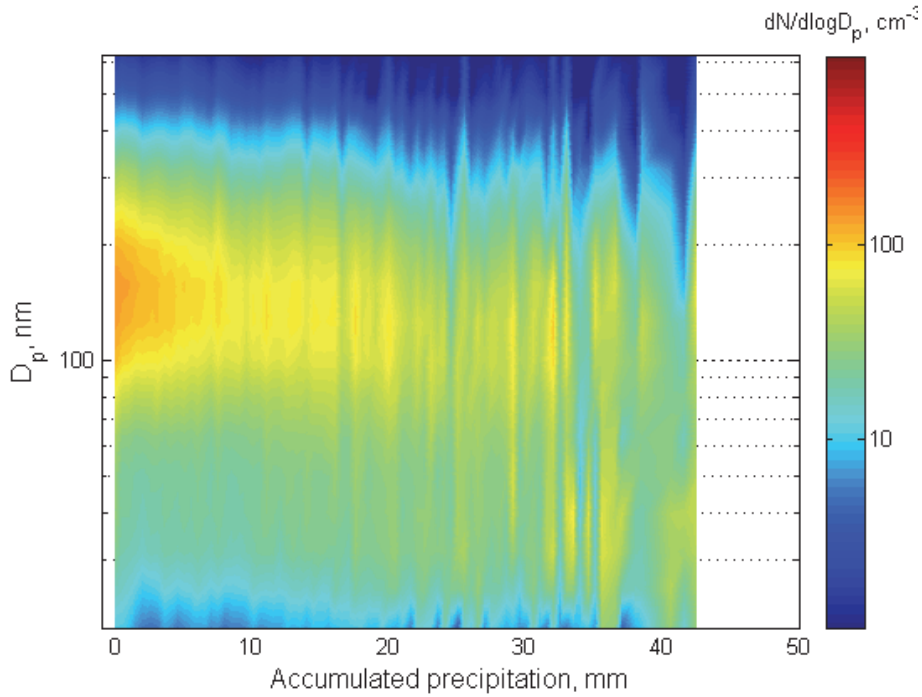

Fig. 17. Evolution of aerosol number size distribution as a function of accumulated precipitation (mm_{tot}) along 240 h trajectories for the dark period (October–February). Data from 2000–2010.

ACPD
12, 29967–30019, 2012

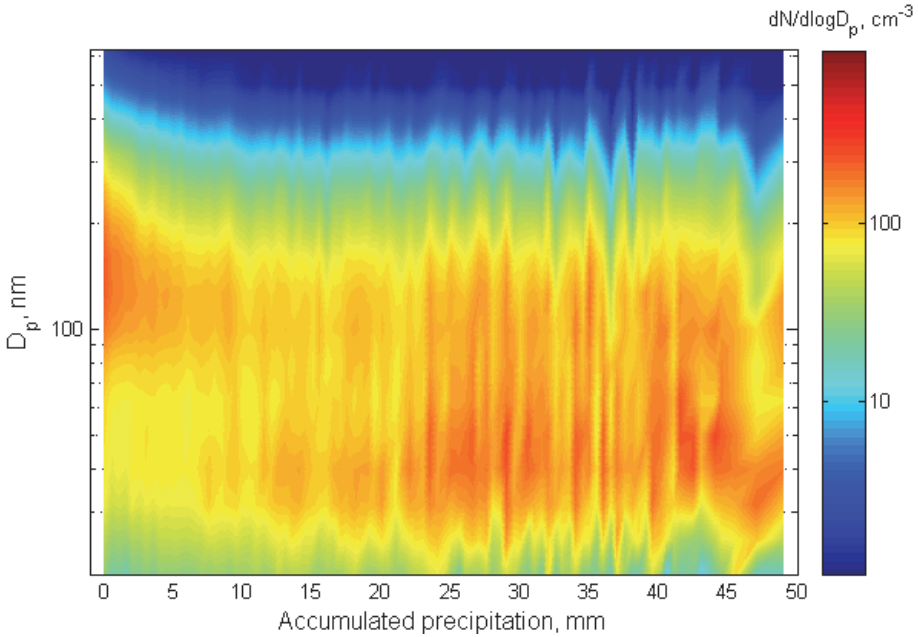

Fig. 18. Evolution of aerosol number size distribution as a function of accumulated precipitation (mm_{tot}) along 240 h trajectories for the sunlit period (March–September). Data from 2000–2010.

ACPD
12, 29967–30019, 2012